Available online at www.sciencedirect.com

SCIENCE DIRECT®

Remote Sensing of Environment 92 (2004) 255–275

Remote Sensing of Environment

www.elsevier.com/locate/rse

Modeling and sensitivity analysis of fire emissions in southern Africa during SAFARI 2000

Stefania Korontzi[a,*], David P. Roy[a,b], Christopher O. Justice[a], Darold E. Ward[c]

[a] Department of Geography, University of Maryland, 2181 LeFrak, College Park, MD 20742, USA
[b] NASA Goddard Space Flight Center, Code 922, Greenbelt, MD 20771, USA
[c] Enviropyronics, LLC, PO Box 968, White Salmon, WA 98672, USA

Received 6 October 2003; received in revised form 3 June 2004; accepted 8 June 2004

Abstract

This paper uses three recently generated southern African satellite burned area products for the month of September 2000 in a sensitivity study of regional biomass burning emissions for a number of trace gases and particulates. Differences in the extent and location of areas burned among products generated from Moderate Resolution Imaging Spectroradiometer (MODIS), Systeme Pour l'Observation de la Terre (SPOT-VEGETATION), and Along Track Scanning Radiometer (ATSR-2) data are significant and result in different emissions estimates for woodland and grassland land cover types. Due to the different emission profiles in woodlands and grasslands, favoring relatively more products of incomplete combustion in woodlands compared with products of complete combustion in grasslands in the late dry season, these changes are not proportional to the differences in the burned area amounts. The importance of accurate burned area information not just in terms of the total area but also in terms of its spatial distribution becomes apparent from our modeling results. This paper highlights the urgent need for satellite data producers to provide accuracy assessments associated with satellite-derived products. Preferably, these accuracy data will be spatially explicit, or defined in a way that can be applied in a spatially explicit modeling context, to enable emissions uncertainties to be defined with respect to different landscape units in support of greenhouse gas emissions reporting.
© 2004 Elsevier Inc. All rights reserved.

1. Introduction

Reliable burned area information is required by a number of users, including global change scientists modeling the source strength, transport, fate, and impacts of trace gas and aerosol emissions from vegetation fires. National governments are required to report their greenhouse gas emissions. Natural resources managers and policy makers can benefit from a synoptic view of fire activity. The savannas of Africa are thought to experience the most extensive biomass burning in the world, for example, contributing an estimated 49% of the carbon lost from fires worldwide (Scholes & Andreae, 2000; Dwyer et al., 2000; Van der Werf et al., 2003). Savanna fires in southern Africa play an important role in the regional atmospheric distribution of trace gases and aerosols, ecosystem functioning, and biogeochemical cycling (Frost & Robertson, 1987; Scholes et al., 1996).

The Southern African Regional Science Initiative (SAFARI 2000) was an international scientific campaign aimed to study land–atmosphere interactions in southern Africa (Swap et al., 2003). One of the main objectives of SAFARI 2000 was the characterization and quantification of regional emissions sources, including those from savanna burning. Within this context, we have developed a spatially explicit emissions model, which we apply here to estimate the pyrogenic emissions for a number of trace gases and particulates during the dry season field campaign in September 2000. In this paper, we perform a sensitivity analysis to examine the geospatial relationship between burned area and emissions. Three recently developed moderate-resolution satellite burned area products from the Moderate Resolution Imaging Spectroradiometer (MODIS), Systeme Pour l'Observation de la Terre (SPOT-VEGETATION), and Along Track Scanning Radiometer (ATSR-2) sensors provide the basis for generating and comparing new estimates of biomass burning emissions from woodland and grassland fires in southern Africa during September 2000. An emissions sensitivity analysis with respect to the woodland–grassland model parameterization is also performed.

* Corresponding author. Tel.: +1-301-4038192.
E-mail address: stef@hermes.geog.umd.edu (S. Korontzi).

0034-4257/$ - see front matter © 2004 Elsevier Inc. All rights reserved.
doi:10.1016/j.rse.2004.06.010

2. Fire emissions modeling methodology

Estimates of pyrogenic gas emissions require information on burned area, fuel load (the amount of fuel per unit area), completeness of combustion (the proportion of the fuel consumed during the fire), and emission factors (characteristic of the amount of the specific atmospheric species produced during the burning). Emissions are computed using spatially explicit input data following the well-established Seiler and Crutzen (1980) model:

$$E_x = \sum_{i,j} A_{i,j} F_{i,j} \mathrm{CC}_{i,j} (\mathrm{EF}_x)_{i,j} \quad (1)$$

where E_x = total pyrogenic emissions for compound x (g); $A_{i,j}$ = burned area (km^2); $F_{i,j}$ = fuel load (kg km^{-2}); $\mathrm{CC}_{i,j}$ = completeness of combustion (fraction); $(\mathrm{EF}_x)_{i,j}$ = emission factor for compound x (g kg^{-1}); i,j = spatial coordinates; and x = compound for which emissions are estimated.

We use Eq. (1) to compute emissions of major and minor gaseous compounds and particulate species for September 2000 for all of Africa south of the equator (not including Madagascar) at a pixel size of 1 km^2. The region is stratified spatially into grassland and woodland areas, and the emissions are computed independently for these two land covers. The relative proportions of woody, grass, and leaf litter fuels determine important aspects of fire behavior, which impact factors including emission factors and the completeness of combustion (Hoffa et al., 1999; Shea et al., 1996). In grasslands, the fuel layer is relatively homogeneous, whereas in woodlands, the woody and grass fuel components coexist with more restricted grass production in the more closed-canopy woodlands (Scholes et al., 2002). We apply different emission factors and combustion completeness estimates for woodlands and grasslands. The Intergovernmental Panel on Climate Change (IPCC) guidelines for greenhouse gas emissions reporting also suggest the division of these two savanna land covers (IPCC, 1997). We use the MODIS percent tree cover (PTC) product (Hansen et al., 2002) to distinguish between grasslands and woodlands, and define areas with PTC less than or equal to 10% as grasslands and areas with PTC greater than 10% as woodlands. The 10% PTC threshold is based on the definition of forest of the Food and Agricultural Organization (FAO) of the United Nations (FAO, 2001). This PTC-based land cover classification is illustrated in Fig. 1. Preliminary validation efforts estimate the global MODIS PTC product accuracy to be ± 11.5%, although local validation in Zambia indicates an accuracy of ± 5.2% (Hansen et al., 2004).

2.1. Model inputs

2.1.1. Burned area

To compare the sensitivity of the emissions estimation to the burned area, three regional moderate spatial resolution burned area products derived from MODIS, SPOT-VEGETATION, and ATSR-2 satellite data are used. The MODIS active fire product is also compared with these products, as prior to the generation of spatially explicit burned area products, active fire locations were the only regional data available for emissions estimation. All datasets were projected into a common Lambert Azimuthal Equal Area projection using nearest-neighbor resampling.

The MODIS burned area product maps the 500-m location and approximate day of burning using a change detection algorithm based on a bidirectional reflectance model-based expectation method applied to the MODIS near-infrared and shortwave infrared bands (Roy et al., 2002b). The algorithm was applied to recently reprocessed 500-m daily MODIS land surface reflectance data to produce burned area datasets for all of southern Africa for 2000 onwards. The MODIS burned area data used in this paper are available on the third SAFARI 2000 CD-ROM (Roy, 2003). In order to minimize geolocation errors associated with nearest-neighbor resampling, the 500-m burned area data were reprojected into the Lambert Azimuthal Equal Area projection with an output pixel dimension of 500 m rather than 1 km. The reprojected data were then binned to 1-km pixels by counting how many burned 500-m pixels occur in each 1-km pixel (zero to four) (i.e., in an 1-km^2 pixel with a count of one, only 25% of the pixel is burned, whereas a 1-km^2 pixel with a count of four is assumed to be completely burned). This reduces nearest-neighbor resampling pixel shifts (i.e., position errors) (Dikshit & Roy, 1996) and provides a more accurate burned area assessment for subsequent analysis. Pixels labeled by the MODIS burned area product as "not considered" (either an area of ephemeral or inland water) or "unmapped" (due to insufficient MODIS data associated with persistent cloud and/or missing MODIS data) were not counted. The precise day of burning may not be certain because of cloudy and missing data. We used a conservative estimate of the area burned in September 2000 by only considering pixels with burns occurring in September and on the last day of the previous month.

The MODIS active fire product maps the 1-km location of active fires detected at the time of satellite overpass using an established contextual hot spot detection algorithm (Justice et al., 2002a). The timing and spatial extent of burning cannot be estimated reliably from these orbital hot spot data, as the satellite may not overpass when burning occurs and because clouds may preclude active fire detection (Justice et al., 1993, 2002a; Robinson, 1991). Despite this limitation, we computed a spatially explicit 1-km September active fire dataset by temporally compositing all the MODIS 1-km day and night September active fire detections over southern Africa. Both the MODIS active fire and burned area products were produced from the latest reprocessed MODIS Collection 4 data (Justice et al., 2002b). We note that MODIS data sensed prior to November 2000 are less reliable compared with later data, due to some noisy and poorly performing MODIS detectors

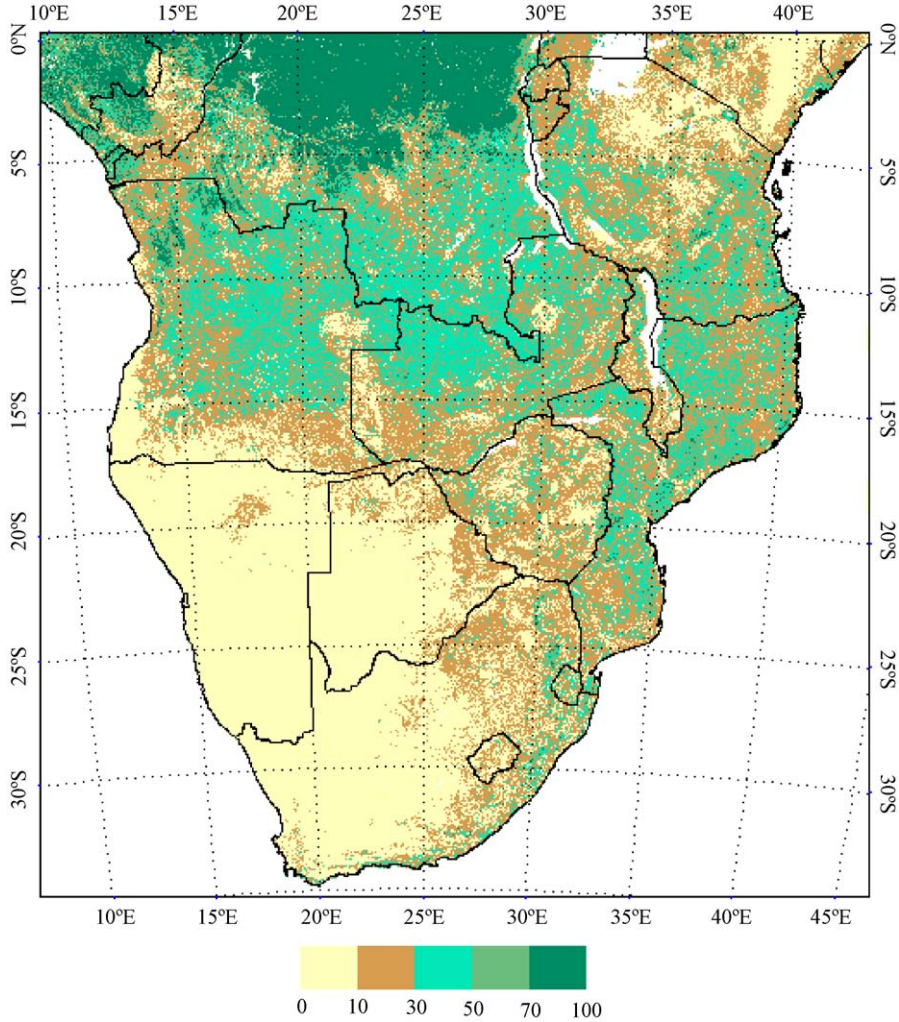

Fig. 1. Southern Africa MODIS PTC product shaded to show the derived woodland–grassland classification. Grasslands (PTC ≤ 10%); woodlands (PTC>10%). Lambert Azimuthal Equal Area projection (center longitude 25°, center latitude −15°).

(Guenther et al., 2002), which had a deleterious impact on MODIS land product quality (Roy et al., 2002a).

Two regional SPOT-VEGETATION burned area products were initially considered; both map the 1-km location and month of burning. The first, produced by application of a supervised classification tree algorithm to 1-km near-infrared SPOT-VEGETATION data (Silva et al., 2003), was superceded by a second SPOT-VEGETATION product computed using a supervised classification tree algorithm applied to the red, near-infrared, and spectral band indices (Tansey et al., 2002). In this paper, we use the second SPOT-VEGETATION burned area product that is more recently distributed as part of Global Burnt Area 2000 (GBA-2000) initiative developed at the Joint Research Centre of the European Commission (Grégoire et al., 2003). We used the September GBA-2000 product and noted that the compositing algorithm used to generate this product (Stroppiana et al., 2002) tends to discard areas that burned on the last 2 days of the month (J. Silva, personal communication, 2003).

The global ATSR-2 burned area product (GLOBSCAR) is based on the logical AND of two independent algorithms—one based on near-infrared reflectance decrease and thermal band brightness temperature increase after a fire (Piccolini, 1998), and the other applying thresholds to spectral band indices and individual ATSR-2 bands (Eva & Lambin, 1998). Preliminary validation activities in southern Africa indicate that the seasonal distribution of burning is well matched, but that there is an underdetection of burning, caused primarily by the joint use of the two algorithms and the relatively low ATSR repeat cycle days interacting with persistent cloud (Simon et al., 2004).

2.1.2. Fuel load

Regional fuel load datasets of green grass, dry grass, leaf litter, and twigs fuel types generated by Hély et al. (2003b) for southern Africa, in support of SAFARI 2000 fire emissions modeling, are used to compute spatially explicit total fuel load amounts and fuel load type

mixtures. The modeled fuel load type outputs used in this paper are available on the third SAFARI 2000 CD-ROM (Hély et al., 2003a). The production of green and dry grass, and leaf litter fuel types is calculated using a satellite-driven net primary productivity (NPP) model that incorporates ecophysiological processes, such as respiration and potential evapotranspiration, in conjunction with empirical relationships. Herbivory reduction of the grass fuel is also included using established mammalian metabolic energy requirement statistics and regional livestock density maps (Hély et al., 2003b). The twigs amount is not explicitly calculated by the NPP model but is determined empirically from an AVHRR-derived PTC. Here, we improve the modeled twigs data layer using the MODIS PTC and the empirical relationship used by Hély et al. (2003b). Fuel amount for each fuel type is computed for each 1-km^2 pixel every 15 days for the preceding growing season from September 1, 1999 to August 31, 2000. The total fuel load available for burning in September 2000 is determined by accumulating fuel load throughout this period. The fuel load ranges predicted by the model are generally in agreement with the limited published field measurements (Hély et al., 2003b; Shea et al., 1996; Trollope et al., 1996). We recognize several potential biases in the fuel load model, including: no modeling of fuel load reduction by people, fuel load accumulation and decay since the last fire occurrence, and larger diameter woody fuels are not modeled even though smoldering following fires on these fuel types may be highly emissive (Bertschi et al., 2003). Investigation of the impact of these limitations is currently not possible since only this particular fuel load dataset is publicly available. We hope that recognition of these issues will lead to the development of more robust fuel load models.

2.1.3. Combustion completeness

Combustion completeness is defined as the fraction burned of the biomass fuel exposed to the fire (Scholes et al., 1996; Shea et al., 1996). Combustion completeness depends on the fuel loading, type, moisture content, packing, and meteorological parameters including wind speed, relative humidity, and temperature. Fine and/or drier fuels typically burn more completely than coarser and/or moister fuels. The combustion completeness of all fuel types is generally thought to increase as the southern African dry season progresses (Hoffa et al., 1999). In grasslands, the combustion completeness is determined from the percentage of green grass to total grass (PGREEN) for values of PGREEN equal or greater than 20%, to allow for the assessment of the effects of varied grass moisture content, and has a lower limit of 44% based on field measurements by Hoffa et al. (1999):

$$CC_{grass} = -213.09 \times PGREEN + 138.21 \quad (2)$$

For values of PGREEN below 20%, CC_{grass} is computed using an empirical relationship derived from the late dry season measurements by Shea et al. (1996) during SAFARI 92:

$$CC_{grass} = (0.99 \times \text{dry grass} + 0.98 \times \text{green grass} + 0.91 \times \text{leaf litter} + 0.48 \times \text{twigs})/\text{total fuel} \quad (3)$$

In woodlands, the combustion completeness is determined from PGREEN for values of PGREEN equal or greater than 14%, and has a lower limit of 1% (Hoffa et al., 1999):

$$CC_{wood} = -114.792 \times PGREEN + 52.704 \quad (4)$$

For PGREEN values below 14%, the CC_{wood} is calculated using Eq. (3).

For the most part, the fuel load model predicted grass is dry in September. For example, in September, PGREEN is typically lower than 20% in grasslands and lower than 14% in woodlands. Consequently, the combustion completeness is mainly computed using Eq. (3) and the combustion is relatively complete.

2.1.4. Emission factors

An emission factor is the amount of a specific trace substance emitted by the combustion per unit mass of dry fuel consumed (g kg^{-1}) (Ward et al., 1996). Regional grassland and woodland emissions are estimated using ecosystem-specific emission factor algorithms for carbon dioxide (CO_2), carbon monoxide (CO), methane (CH_4), nonmethane hydrocarbons (NMHCs), and particulate matter with diameter less than 2.5 μm ($PM_{2.5}$) for southern African savanna fires (Korontzi et al., 2003b). Most modeling studies report emissions for these key five carbon-containing species. Here, we expand the emission database for this region by incorporating emission factors for a variety of compounds, including oxygenated volatile organic compounds (OVOCs), halocarbons, nitrogen oxides (NO_x), ammonia (NH_3), sulfur dioxide (SO_2), hydrogen cyanide (HCN), and particulate ionic components measured during the SAFARI 2000 dry season field campaign (Sinha et al., 2003; Yokelson et al., 2003). A fuel carbon content of 50% is assumed in all emission factors calculations (Ward et al., 1996). The term "products of incomplete combustion" is used to describe compounds reported in this study other than CO_2 and NO_x (i.e., low oxidized emissions products that are mainly emitted during smoldering combustion).

Emission factors are usually computed as a linear function of the modified combustion efficiency (MCE) for a given fuel type (Ward et al., 1996). The MCE is an index of the fire oxidation conditions, defined as the molar ratio of carbon emitted as CO_2 to the sum of carbon emitted as CO

and CO_2. In this work, we use models of emission factors versus MCE reported in the literature for southern Africa fuels (Korontzi et al., 2003b; Sinha et al., 2003; Ward et al., 1996; Yokelson et al., 2003). For woodlands, we compute MCE_{wood} from the ratio of the grass fuel to the sum of grass and litter fuels (Ward et al., 1996):

$$MCE_{wood} = 0.85 + 0.11[\text{grass}/(\text{litter} + \text{grass})]^{0.34} \quad (5)$$

"Grass" consists of green and dry grass. "Litter" consists of fallen tree leaves and twigs.

For grasslands, we compute the MCE_{grass} from PGREEN constrained by a lower limit of 0.912 and an upper limit of 0.974 (Hoffa et al., 1999; Korontzi et al., 2003b):

$$MCE_{grass} = 1.010 - 0.217 \times \text{PGREEN} \quad (6)$$

In grassland locations dominated by litter (e.g., where grass has been removed by herbivory), MCE_{grass} is set to 0.85 (Ward et al., 1996). These locations comprised small fractions of the grassland burned area (approximately 6% of the GBA-2000, 6% of MODIS, and 9% of the GLOBSCAR September grassland burned areas). As seen from Eqs. (5) and (6), the MCE varies as the vegetation condition changes. Thus, the emission factor algorithms provide a means of estimating the proportion of different compounds in the smoke mixture at any temporally and spatially defined pixel.

3. Results and discussion

3.1. Intercomparison of MODIS, GBA-2000, and GLOBSCAR burned area products, southern Africa, September 2000

Tables 1 and 2 summarize the regional differences between the MODIS, GBA-2000, and GLOBSCAR burned area products for September 2000. The total southern African area considered is 9,269,225 km^2. MODIS detects a regional September burned area amount of approximately 268,500 km^2, GBA-2000 detects approximately 173,100 km^2, and GLOBSCAR detects approximately 59,800 km^2. The MODIS active fire product detects an approximate area of 126,400 km^2, although as we noted above, this estimate is expected to be biased.

Table 1
MODIS and GBA-2000 burned area product intercomparison, southern Africa, September 2000

	Burned area (km$^2 \times 10^3$)
Total MODIS	268.5[a]
Total GBA	173.1[b]
Detected by MODIS but not GBA	181.6[a]
Detected by GBA but not MODIS	60.4[b]
Detected by GBA, not mapped by MODIS	5.9[b]
Detected by both MODIS and GBA	86.9[a], 106.8[b]

All burned areas to the nearest 100 km^2.
[a] The burned areas are defined with respect to MODIS 500-m pixels.
[b] The burned areas are defined with respect to 1-km GBA-2000 pixels.

Table 2
MODIS and GLOBSCAR burned area product intercomparison, southern Africa, September 2000

	Burned area (km$^2 \times 10^3$)
Total MODIS	268.5[a]
Total GLOBSCAR	59.8[b]
Detected by MODIS but not GLOBSCAR	254.4[a]
Detected by GLOBSCAR but not MODIS	33.7[b]
Detected by GLOBSCAR, not mapped by MODIS	6.2[b]
Detected by both MODIS and GLOBSCAR	14.1[a], 19.9[b]

All burned areas to the nearest 100 km^2.
[a] The burned areas are defined with respect to MODIS 500-m pixels.
[b] The burned areas are defined with respect to 1-km GBA-2000 pixels.

Spatially explicit comparisons of these products are shown in Figs. 2 and 3, and illustrate the large differences between products. Pixels labeled by the MODIS burned area product as "unmapped" (due to insufficient data associated with persistent cloud and/or missing data) are shown as light grey. The GBA-2000 and GLOBSCAR products are defined without an unmapped class, potentially increasing the possibility of burned areas being mapped as unburned rather than unmapped due to missing, infrequent, and/or cloudy data.

The MODIS product mapped a total burned area approximately 1.5 times greater than GBA-2000, and of the 173,100 km^2 mapped by GBA-2000, the summed area of GBA-2000 1-km pixels containing one or more 500-m MODIS burned pixels is 106,800 km^2 (Table 1). Calculating the coincident area with respect to the MODIS data gives a smaller common area of 86,900 km^2 because many of the burned 1-km GBA-2000 pixels contain less than four 500-m MODIS burned pixels. Systematic differences are also present. For example, the GBA-2000 product has discontinuous linear stripes of burned pixels hundreds of kilometers long aligned in the SPOT orbit that are probably artifacts (although negligible for this analysis) and has extensive burning in the Kenya–Tanzania border (Fig. 2) that are not found in the MODIS or GLOBSCAR products. The MODIS product mapped an area more than four times greater than GLOBSCAR, and of the 59,800 km^2 mapped by GLOBSCAR, less than 20,000 km^2 were coincidentally mapped by MODIS (Table 2).

Table 3 tabulates the total area burned for the three products broken down by woodlands and grasslands, as these land covers are used to parameterize our emissions model. Woodland fires (defined as PTC>10%) account for the majority of the regional burned area rather than grassland fires (defined as PTC ≤ 10%). MODIS and GBA-2000 map similar burned areas in grasslands and approximately six times more than GLOBSCAR. MODIS maps approxi-

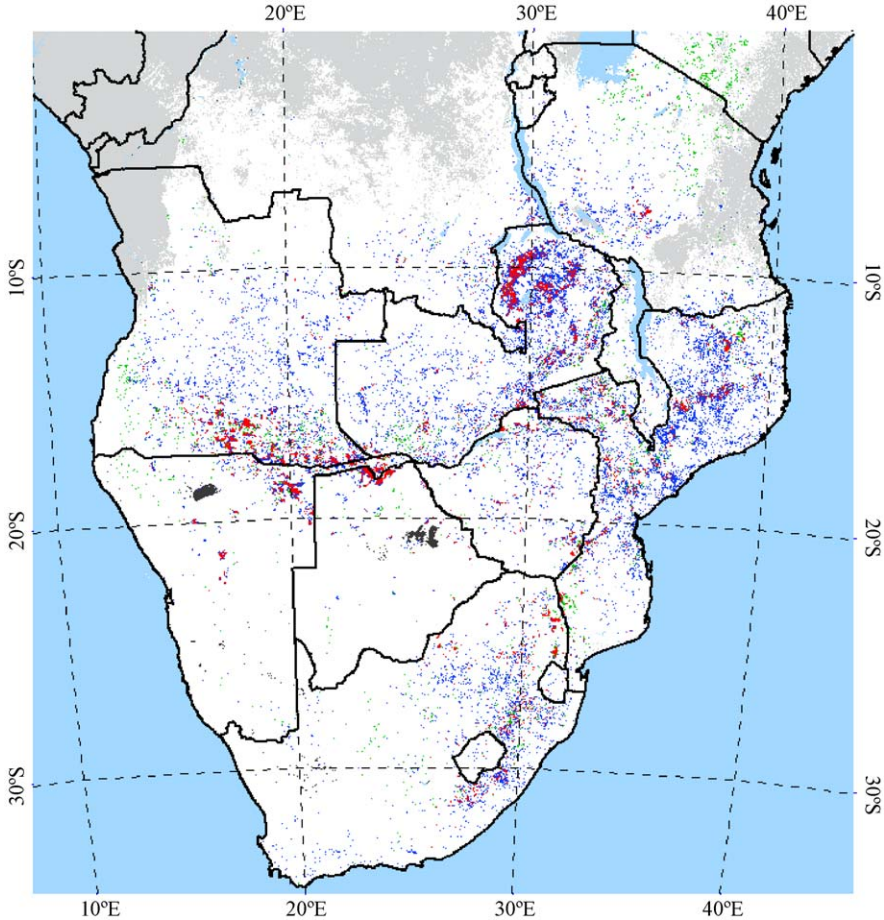

Fig. 2. Intercomparison of the MODIS and GBA-2000 burned area products, southern Africa, September 2000. Dark blue = MODIS detections only; light green = GBA-2000 detections only; red = agreement; light grey = not mapped by MODIS due to insufficient cloud-free observations; dark grey = not considered by MODIS due to ephemeral water or inland water; light blue = water. Lambert Azimuthal Equal Area projection (center longitude 25°, center latitude −15°).

mately twice as much burned area in woodlands as GBA-2000, which maps approximately twice as much burned area in woodlands as GLOBSCAR. The ratio of woodland to grassland burned area varies among products. GLOBSCAR presents the highest relative proportion of woodland burns (~83%), followed by MODIS (~75%), and then GBA-2000 (~66%). Fig. 4 illustrates the regional amount of area burned as a function of PTC greater than 10% for each burned area dataset. MODIS detects a proportionally higher burned area than GBA-2000 or GLOBSCAR for PTC 40–50% and always has higher area burned up to 60% PTC. Both MODIS and GBA-2000 have approximately bimodal distributions with peaks at approximately 20% and 30% PTC, indicating that they detect a similar regional distribution of woodland burning. The GLOBSCAR product has a uniform burned area distribution up to approximately 50% PTC and then decreases in a similar manner as the other burned area datasets.

None of the three 2000 satellite burned area products has been systematically validated. The extent to which differences among these products are due to commission and omission errors is unknown. Consequently, it is difficult to reliably explain differences observed between them, especially as different algorithms were used in their generation. All factors being equal, higher spatial resolution systems will more reliably detect burned areas (i.e., have lower omission errors) than lower spatial resolution systems. This is because increasing the fraction of the observation area (sensed by a pixel) that burns increases the change in reflectance that occurs after the passage of fire, and thus the detection likelihood (Roy & Landmann, in press). Similarly, higher spatial resolution data may allow more reliable detection of burned surfaces that are partially obscured by unburned overstorey vegetation, which are more common in dense woodlands. These factors may, in part, explain the more extensive burning detected using 500-m MODIS data than that detected by the 1-km SPOT-VEGETATION (GBA-2000) and the ATSR-2 (GLOBSCAR). Recent validation of the improved-quality MODIS 2001 and 2002 burned area product, performed using Landsat ETM+-derived independent burned area data (Roy et al., in press), indicates that the MODIS burned area is underestimating the regional area burned (Roy et al., 2003). We note that calibration, data

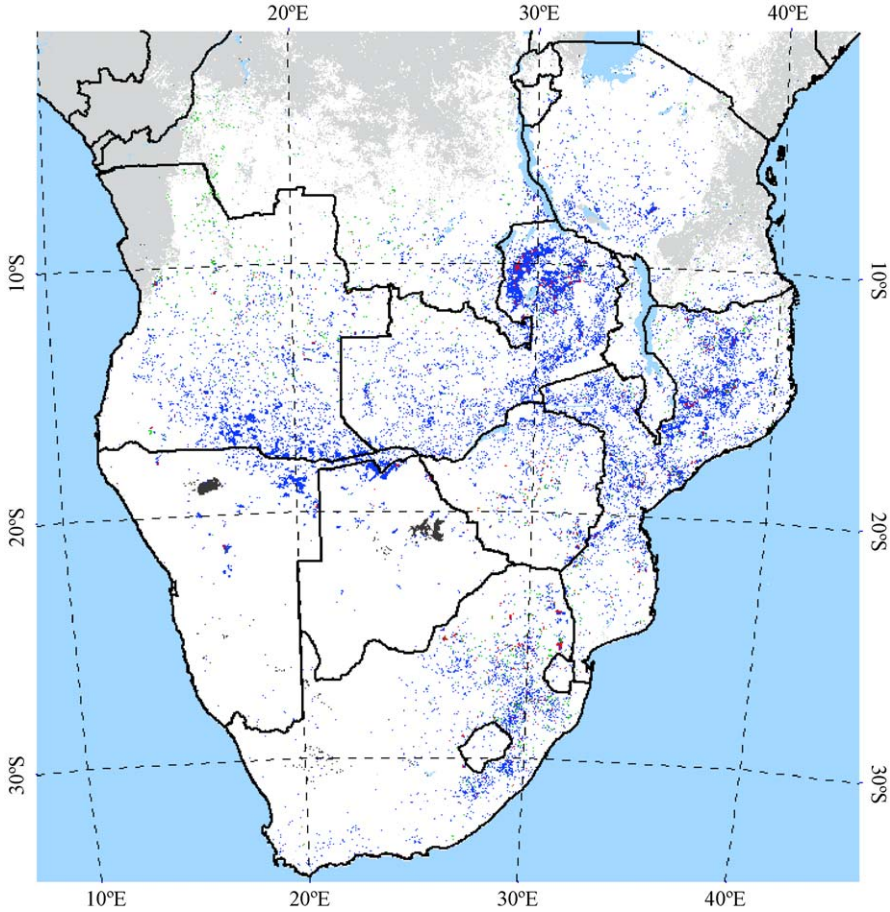

Fig. 3. Intercomparison of the MODIS and GLOBSCAR burned area products, southern Africa September 2000. Dark blue = MODIS detections only; light green = GLOBSCAR detections only; red = agreement; light grey = not mapped by MODIS due to insufficient cloud-free observations; dark grey = not considered by MODIS due to ephemeral water or inland water; light blue = water. Lambert Azimuthal Equal Area projection (center longitude 25°, center latitude −15°).

preprocessing, spectral characteristics, and algorithm differences may also be highly important factors. As the purpose of this paper is an emissions sensitivity analysis, we are less concerned with why the burned area datasets are different and more concerned with the impact of the observed differences.

3.2. Sensitivity of regional fire emissions to MODIS, GBA-2000, and GLOBSCAR

Figs. 5 and 6 illustrate the September 2000 MODIS-based carbon dioxide (CO_2) and carbon monoxide (CO) emission densities (emissions per unit area). Intense, efficient (flaming) fires have more complete combustion and release more CO_2, whereas less efficient (smoldering) fires have less

Table 3
MODIS, GBA-2000, and GLOBSCAR burned areas in woodlands and grasslands

Burned area ($km^2 \times 10^3$)	Woodlands	Grasslands	Ratio (woodlands/grasslands)
MODIS	201.6	66.9	3.0
GBA-2000	113.9	59.2	1.9
GLOBSCAR	49.6	10.2	4.9

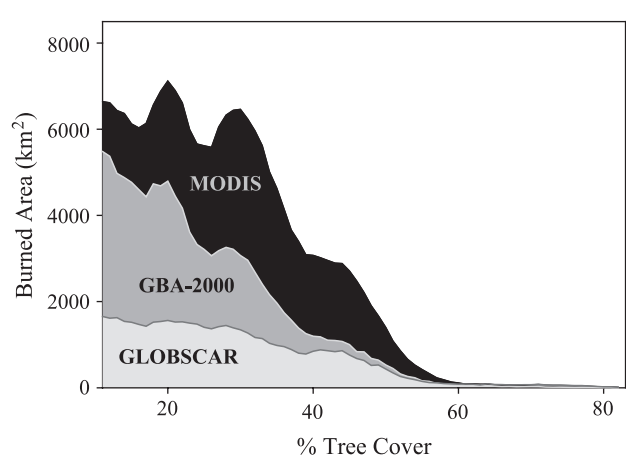

Fig. 4. Distribution of burned area in woodlands in the MODIS, GBA-2000, and GLOBSCAR products by PTC for southern Africa, September 2000. The distributions are binned at 1% PTC intervals, starting at 11% PTC.

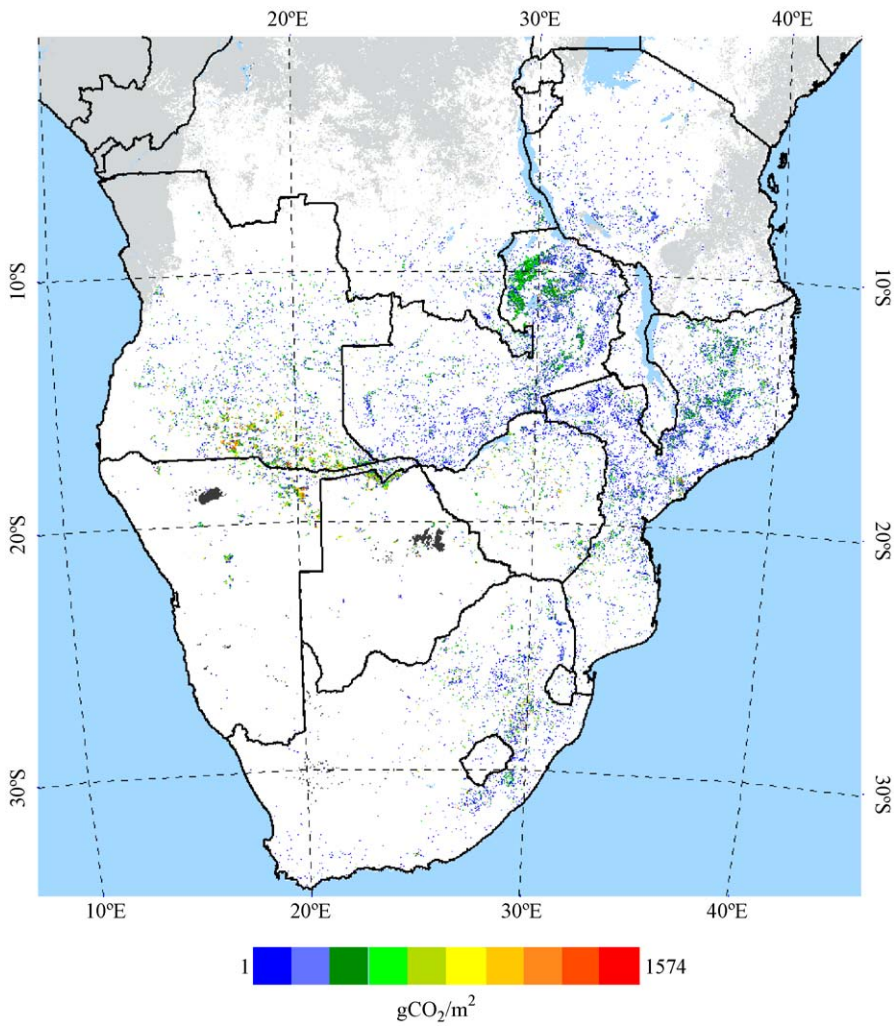

Fig. 5. MODIS CO_2 emissions, southern Africa, September 2000. Light grey = not mapped by MODIS due to insufficient cloud-free observations; dark grey = not considered by MODIS due to ephemeral water or inland water; light blue = water. Lambert Azimuthal Equal Area projection (center longitude 25°, center latitude −15°).

complete combustion and release more CO (Ward et al., 1996). There are distinct differences between the spatial distribution of the estimated CO_2 and CO emissions. The highest CO_2 emission densities are concentrated in the latitudinal belt between approximately 15°S and 20°S, whereas the highest CO emission densities are observed between 8°S and 13°S. Examination of the MODIS PTC product reveals that areas with the highest CO_2 emission densities are grasslands and/or open woodlands, whereas areas with the highest CO have higher PTC. The GBA-2000 CO_2 latitudinal distribution is comparable with MODIS, but due to the more disperse burning in GBA-2000, there are no clear latitudinal belts of concentrated high CO emissions. For the same reason, there are no obvious latitudinal trends in the CO_2 and CO regional distribution in GLOBSCAR.

Tables 4–6 summarize the regional September 2000 pyrogenic emissions for major and minor trace gases and particulate species computed using the MODIS (Table 4), the GBA-2000 (Table 5), and the GLOBSCAR (Table 6) products. The regional pyrogenic emissions are highly sensitive to the burned area amounts. For example, the MODIS-driven emissions estimate for CO_2 is approximately 134 Tg, the GBA-2000 emissions estimate is 90 Tg, and the GLOBSCAR estimate is 30 Tg.

Table 7 shows the regional amounts of biomass burned in woodlands and grasslands. The main difference between MODIS and GBA-2000 in terms of burned area (Table 3) and biomass burned (Table 7) is associated with woodland rather than grassland fires. GLOBSCAR detects substantially less burned area and biomass burned in both woodlands and grasslands compared with MODIS and GBA-2000, and the largest differences are found in the grasslands. In MODIS and GBA-2000, more biomass is burned in grasslands than woodlands relative to their respective burned area amounts. In GLOBSCAR, the ratio of biomass burned woodlands over grasslands is slightly higher than the corresponding burned area ratio. Fig. 7a–c illustrates the regional amounts of biomass burned, CO_2, and CO emis-

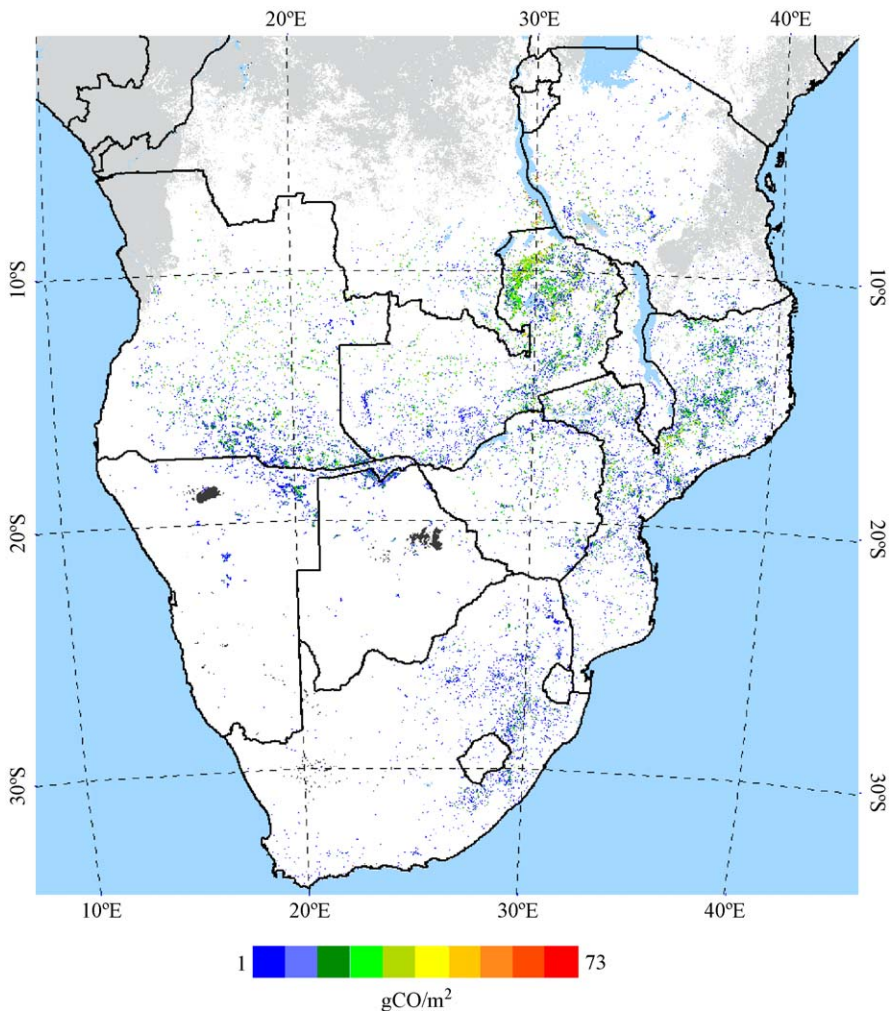

Fig. 6. MODIS CO emissions, southern Africa, September 2000. Light grey = not mapped by MODIS due to insufficient cloud-free observations; dark grey = not considered by MODIS due to ephemeral water or inland water; light blue = water. Lambert Azimuthal Equal Area projection (center longitude 25°, center latitude −15°).

sions in woodlands as a function of PTC. The distribution of the biomass burned by PTC for all three products is similar to that of the burned area (Fig. 4). The CO_2 emission distribution also closely follows that of the biomass and area burned distribution. The CO emissions are different in that they increase up to approximately 30% PTC before decreasing in the same way as CO_2, and biomass burned. We hypothesize that this is because of increasing litter fuel load for PTC up to 30% and then decreasing total biomass burned at higher PTC.

Vegetation burning in the grasslands and woodlands emits various quantities of different atmospheric species that are not necessarily proportional to their correspondent burned area. In MODIS, whereas woodland fires account for approximately 75% of the regional area burned, they contribute approximately 70% of the regional CO_2, 73% of the regional NO_x, and anywhere from 77% to 98% of the regional budgets for the remaining trace gas and particulate species (Table 4). In GBA-2000, woodland fires account for approximately 66% of the regional area burned, but they contribute approximately 60% of the regional CO_2, 63% of the regional NO_x, and anywhere from 67% to 97% of the regional budgets for products of incomplete combustion (Table 5). In GLOBSCAR, woodland fires account for approximately 83% of the regional area burned, and they contribute approximately 82% of the regional CO_2, 79% of the regional NO_x, and anywhere from 87% to 98% of the regional budgets for products of incomplete combustion (Table 6).

Furthermore, when comparing the differences in regional emissions arising from using the different burned area products, it is also evident that they are not directly proportional to differences in burned area amounts between products and that they vary among atmospheric species (Tables 1, 2 and 4–6). The approximately 55% regional increase in burned area detected by MODIS compared with GBA-2000 (Table 1) results in a proportionally smaller increase in emissions of products of complete combustion, such as CO_2 (48%) and NO_x (52%), compared with the emissions of products of incomplete combustion, such as CO (73%) and CH_4 (87%) (Tables 4 and 5). The MODIS-based emissions of the

Table 4
MODIS-based regional fire emissions, southern Africa, September 2000

Species[a]	Woodland	Grassland	Regional
Carbon dioxide (CO_2)	93,393	40,387	133,780
Carbon monoxide (CO)	5100	767	5867
Methane (CH_4)	174.8	13.3	188.1
Nonmethane hydrocarbons (NMHCs)	137.9	20.5	158.4
Nitrogen oxides (as NO)	189.8	70.1	259.9
Dimethyl sulfide (CH_3SCH_3)	0.146	0.036	0.182
Methyl bromide (CH_3Br)	0.089	0.013	0.102
Methyl chloride (CH_3Cl)	4.6	1.3	5.9
Methyl iodide (CH_3I)	0.101	0.029	0.13
Methyl nitrate (CH_3ONO_2)	0.027	0.004	0.031
Ethane (C_2H_6)	12.9	1.9	14.8
Ethene (C_2H_4)	44.6	6.6	51.2
Propane (C_3H_8)	3.882	0.574	4.456
Propene (C_3H_6)	14.443	0.682	15.125
Acetylene (C_2H_2)	12.5	1.8	14.3
i-Butane (*i*-C_4H_{10})	0.2321	0.0055	0.2376
n-Butane (*n*-C_4H_{10})	1.249	0.185	1.434
t-2-Butene (C_4H_8)	1.249	0.185	1.434
1-Butene (C_4H_8)	3.005	0.299	3.304
c-2-Butene (C_4H_8)	0.892	0.132	1.024
i-Pentane (*i*-C_5H_{12})	0.134	0.02	0.154
n-Pentane (*n*-C_5H_{12})	0.55	0.11	0.66
1, 3-Butadiene (C_4H_6)	3.897	0.431	4.328
3-Methyl-1-butene (C_5H_{10})	0.446	0.066	0.512
t-2-Pentene (C_5H_{10})	0.2321	0.0055	0.2376
2-Methyl-2-butene (C_5H_{10})	0.446	0.066	0.512
2-Methyl-1-butene (C_5H_{10})	0.491	0.073	0.564
Isoprene (C_5H_8)	3.109	0.605	3.714
n-Heptane (C_7H_{16})	0.937	0.139	1.076
Benzene (C_6H_6)	12.9	1.9	14.8
Toluene (C_7H_8)	9.4	1.4	10.8
Formaldehyde (HCHO)	75	14.4	89.4
Methanol (CH_3OH)	89	11.6	100.6
Acetic acid (CH_3COOH)	185.5	23.1	208.6
Formic acid (HCOOH)	48.4	11	59.4
Ammonia (NH_3)	18.8	3.4	22.2
Hydrogen cyanide (HCN)	33.4	10	43.4
Particulates with diameter < 2.5 μm ($PM_{2.5}$)	586.9	44.4	631.3
Total particulate matter (TPM)	1077	101	1178
Organic carbon (OC)	221.6	47.3	268.9
Black carbon (BC)	25.9	3.8	29.7
Chloride (Cl^-)	117.5	2.9	120.4
Nitrate (NO_3^-)	16.4	3.9	20.3
Sulfate (SO_4^{2-})	18.4	1.3	19.7
Potassium (K^+)	71.4	10.6	82

[a] Values are in gigagrams (10^9 g).

products of incomplete combustion are higher by approximately 57–98% compared with the GBA-2000 equivalents. Comparison of MODIS with GLOBSCAR yields the opposite results. The MODIS burned area product maps approximately 349% more area burned than the GLOBSCAR product (Table 2). In this case, MODIS CO_2 and NO_x emissions are higher by approximately 341% and 338% than the corresponding GLOBSCAR emissions, respectively (Tables 4 and 6). The MODIS-based emissions of products of incomplete combustion are higher by mostly smaller proportions than CO_2 and NO_x, ranging from 310% to 336%, compared with the respective GLOBSCAR-based emissions. Examination of Eqs. (1)–(6) indicates that burned area differences will produce different emissions estimates, and that these differences will be dependent on the spatial distribution of burning relative to the fuel load amount and composition in grasslands and woodlands.

To address the effects of the different spatial distribution of the three burned area products on emissions and to verify the model's behavior toward the various burned area inputs, we examine the variations in fuel load density, biomass

Table 5
GBA-2000-based regional fire emissions, southern Africa, September 2000

Species[a]	Woodlands	Grasslands	Regional
Carbon dioxide (CO_2)	53,935	36,320	90,255
Carbon monoxide (CO)	2711	680	3391
Methane (CH_4)	89.2	11.6	100.8
Nonmethane hydrocarbons (NMHCs)	74.8	17.8	92.6
Nitrogen oxides (as NO)	107.6	63.0	170.6
Dimethyl sulfide (CH_3SCH_3)	0.079	0.032	0.111
Methyl bromide (CH_3Br)	0.047	0.017	0.064
Methyl chloride (CH_3Cl)	2.5	1.1	3.6
Methyl iodide (CH_3I)	0.056	0.026	0.082
Methyl nitrate (CH_3ONO_2)	0.0142	0.0035	0.0177
Ethane (C_2H_6)	6.9	1.7	8.6
Ethene (C_2H_4)	23.7	5.8	29.5
Propane (C_3H_8)	2.060	0.509	2.569
Propene (C_3H_6)	7.420	0.576	7.996
Acetylene (C_2H_2)	6.6	1.6	8.2
i-Butane (*i*-C_4H_{10})	0.1161	0.0042	0.1203
n-Butane (*n*-C_4H_{10})	0.663	0.164	0.827
t-2-Butene (C_4H_8)	0.663	0.164	0.827
1-Butene (C_4H_8)	1.571	0.262	1.833
c-2-Butene (C_4H_8)	0.474	0.117	0.591
i-Pentane (*i*-C_5H_{12})	0.071	0.018	0.089
n-Pentane (*n*-C_5H_{12})	0.297	0.098	0.395
1, 3-Butadiene (C_4H_6)	2.044	0.379	2.423
3-Methyl-1-butene (C_5H_{10})	0.237	0.058	0.295
t-2-Pentene (C_5H_{10})	0.1161	0.0042	0.1203
2-Methyl-2-butene (C_5H_{10})	0.237	0.058	0.295
2-Methyl-1-butene (C_5H_{10})	0.260	0.064	0.324
Isoprene (C_5H_8)	1.673	0.539	2.212
n-Heptane (C_7H_{16})	0.497	0.123	0.62
Benzene (C_6H_6)	6.9	1.7	8.6
Toluene (C_7H_8)	5.0	1.2	6.2
Formaldehyde (HCHO)	40.4	12.8	53.2
Methanol (CH_3OH)	47.0	10.3	57.3
Acetic acid (CH_3COOH)	97.8	20.4	118.2
Formic acid (HCOOH)	26.3	9.8	36.1
Ammonia (NH_3)	10.1	3.0	13.1
Hydrogen cyanide (HCN)	18.6	9.0	27.6
Particulates with diameter < 2.5 μm ($PM_{2.5}$)	295.3	39.3	334.6
Total particulate matter (TPM)	562.0	88.5	650.5
Organic carbon (OC)	120.0	42.2	162.2
Black carbon (BC)	13.7	3.4	17.1
Chloride (Cl^-)	60.0	2.2	62.2
Nitrate (NO_3^-)	8.9	3.5	12.4
Sulfate (SO_4^{2-})	9.6	1.1	10.7
Potassium (K^+)	37.9	9.4	47.3

[a] Values are in gigagrams (10^9 g).

Table 6
GLOBSCAR-based regional fire emissions, southern Africa, September 2000

Species[a]	Woodlands	Grassland	Regional
Carbon dioxide (CO_2)	24,951	5368	30,319
Carbon monoxide (CO)	1284	109	1393
Methane (CH_4)	42.8	2.0	44.8
Nonmethane hydrocarbons (NMHCs)	35.2	3.1	38.3
Nitrogen oxides (as NO)	50.0	9.4	59.4
Dimethyl sulfide (CH_3SCH_3)	0.037	0.0049	0.0419
Methyl bromide (CH_3Br)	0.022	0.0019	0.0239
Methyl chloride (CH_3Cl)	1.184	0.170	1.354
Methyl iodide (CH_3I)	0.026	0.0040	0.03
Methyl nitrate (CH_3ONO_2)	0.0067	0.0006	0.0073
Ethane (C_2H_6)	3.255	0.271	3.526
Ethene (C_2H_4)	11.223	0.935	12.158
Propane (C_3H_8)	0.976	0.081	1.057
Propene (C_3H_6)	3.550	0.116	3.666
Acetylene (C_2H_2)	3.142	0.262	3.404
i-Butane (*i*-C_4H_{10})	0.0560	0.0012	0.0572
n-Butane (*n*-C_4H_{10})	0.314	0.026	0.34
t-2-Butene (C_4H_8)	0.314	0.026	0.34
1-Butene (C_4H_8)	0.748	0.045	0.793
c-2-Butene (C_4H_8)	0.224	0.019	0.243
i-Pentane (*i*-C_5H_{12})	0.0337	0.0028	0.0365
n-Pentane (*n*-C_5H_{12})	0.140	0.015	0.155
1,3-Butadiene (C_4H_6)	0.972	0.063	1.035
3-Methyl-1-butene (C_5H_{10})	0.112	0.0093	0.1213
t-2-Pentene (C_5H_{10})	0.0560	0.0012	0.0572
2-Methyl-2-butene (C_5H_{10})	0.1122	0.0093	0.1215
2-Methyl-1-butene (C_5H_{10})	0.123	0.010	0.133
Isoprene (C_5H_8)	0.790	0.084	0.874
n-Heptane (C_7H_{16})	0.236	0.020	0.256
Benzene (C_6H_6)	3.255	0.271	3.526
Toluene (C_7H_8)	2.357	0.196	2.553
Formaldehyde (HCHO)	19.1	2.0	21.1
Methanol (CH_3OH)	22.3	1.7	24
Acetic acid (CH_3COOH)	46.4	3.3	49.7
Formic acid (HCOOH)	12.4	1.5	13.9
Ammonia (NH_3)	4.764	0.469	5.233
Hydrogen cyanide (HCN)	8.7	1.4	10.1
Particulates with diameter <2.5 μm ($PM_{2.5}$)	142.2	6.3	148.5
Total particulate matter (TPM)	267.7	15.1	282.8
Organic carbon (OC)	56.5	6.5	63
Black carbon (BC)	6.509	0.542	7.051
Chloride (Cl^-)	28.767	0.600	29.367
Nitrate (NO_3^-)	4.194	0.529	4.723
Sulfate (SO_4^{2-})	4.560	0.200	4.76
Potassium (K^+)	18.0	1.5	19.5

[a] Values are in gigagrams (10^9 g).

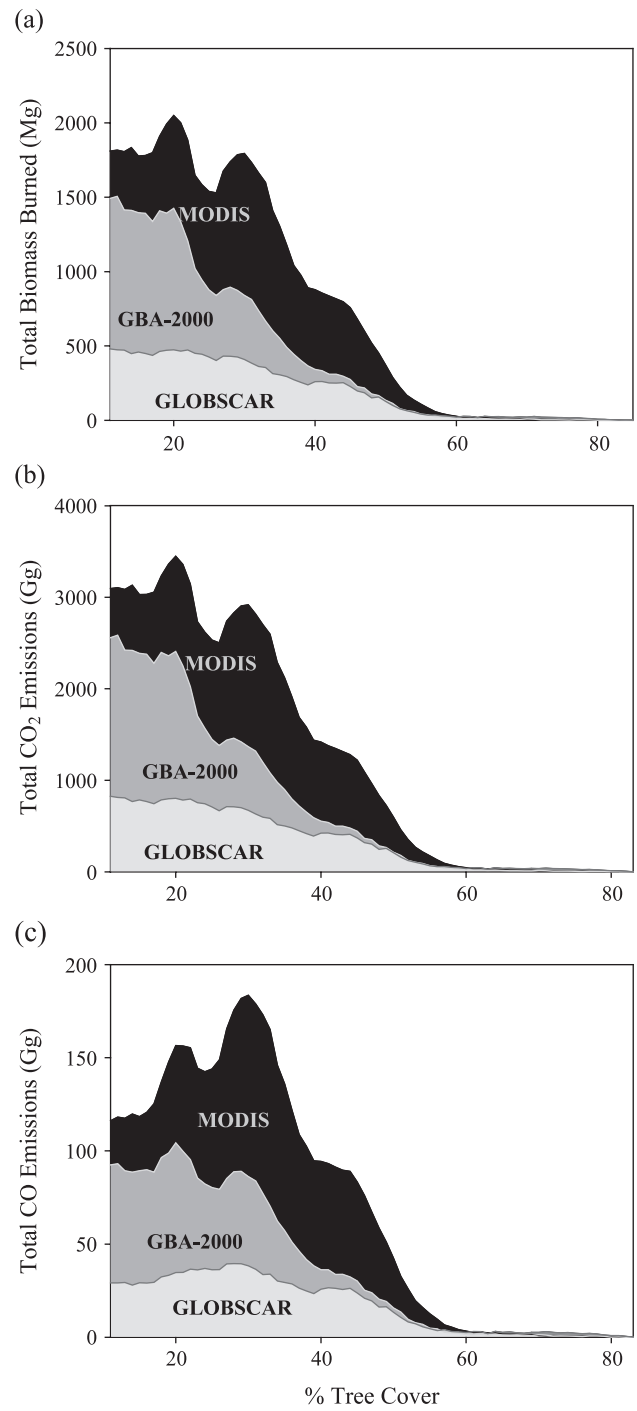

Fig. 7. Southern Africa, September 2000, distributions by PTC of (a) biomass burned, (b) CO_2 emissions, and (c) CO emissions in woodland fires. The distributions are binned at 1% PTC intervals, starting at 11% PTC.

Table 7
MODIS, GBA-2000, and GLOBSCAR biomass burned in woodlands and grasslands

Biomass burned (Tg)	Woodlands	Grasslands	Total	Ratio (woodlands/grasslands)
MODIS	56.5	22.9	79.4	2.5
GBA-2000	32.4	20.6	53.0	1.6
GLOBSCAR	15.0	3.0	18.0	5

burned density, combustion completeness, emission factors for CO_2 ($EFCO_2$) and CO (EFCO), and CO_2 and CO emission densities for each burned area product. Figs. 8–10 show for MODIS, GBA-2000, and GLOBSCAR, respectively, the variations in these variables as a function of PTC defined within 5% PTC ranges. The suppressive effect of increasing PTC on grass production is apparent in Figs.

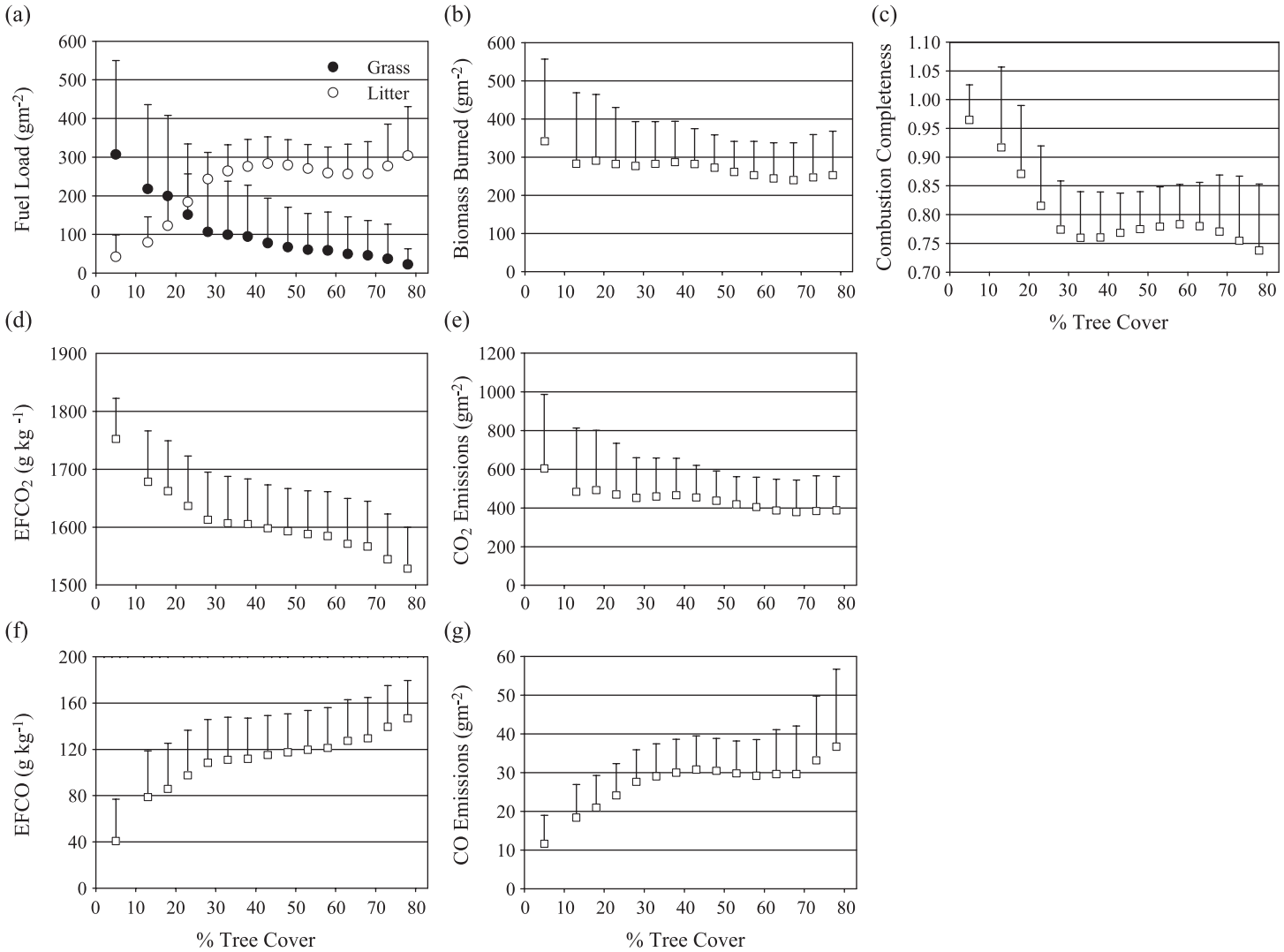

Fig. 8. Mean (symbol) and 1 S.D. statistics computed from the southern Africa, September 2000, MODIS burned area pixels of (a) fuel load, (b) biomass burned, (c) combustion completeness, (d) CO_2 emission factors, (e) CO_2 emissions, (f) CO emission factors, and (g) CO emissions. The grassland ($0\% \leq PTC \leq 10\%$) statistics are shown at PTC = 5%. The woodland (PTC>10%) statistics are defined over 5% PTC intervals.

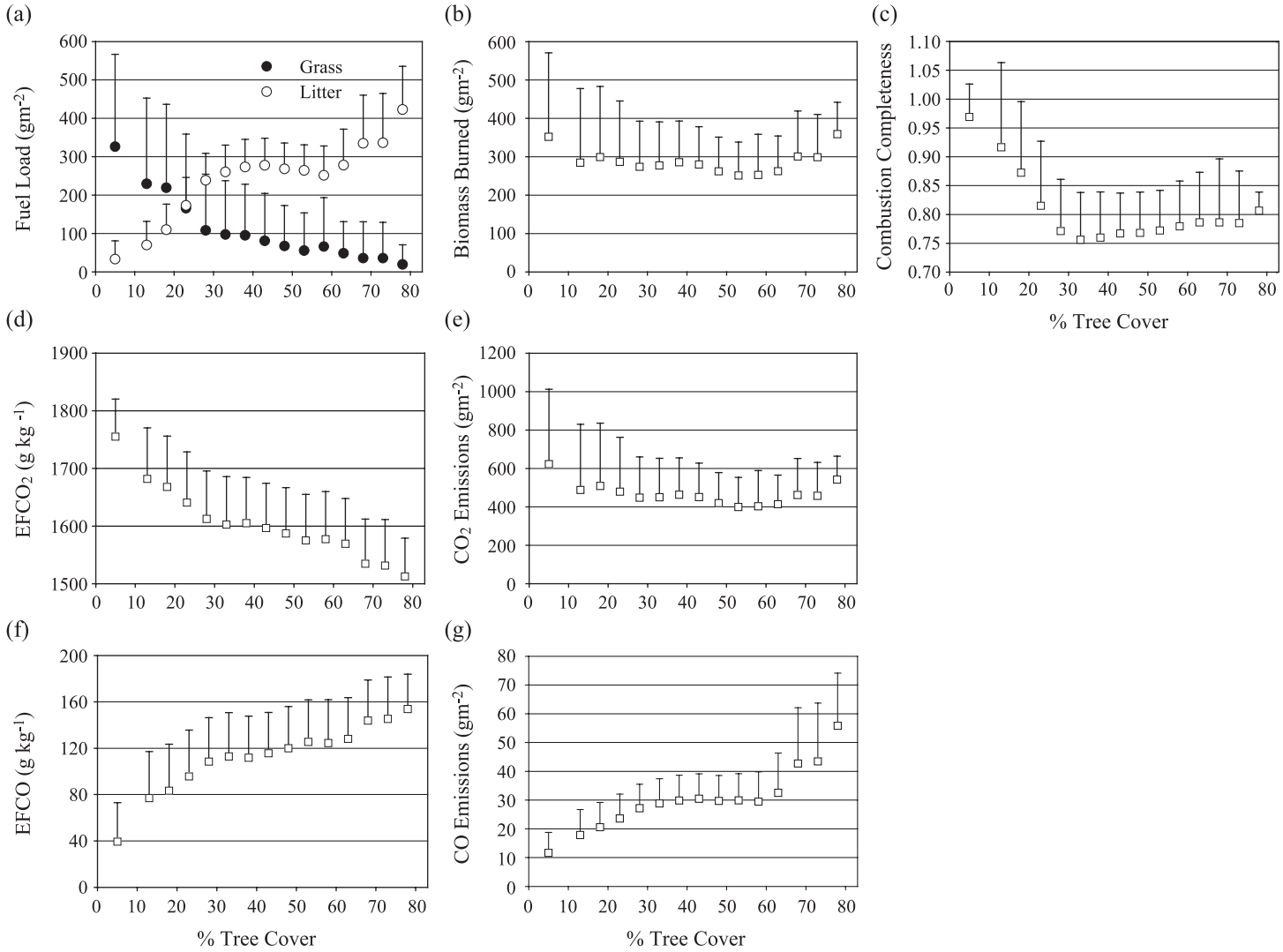

Fig. 9. Mean (symbol) and 1 S.D. statistics computed from the southern Africa, September 2000, GBA-2000 burned area pixels of (a) fuel load, (b) biomass burned, (c) combustion completeness, (d) CO_2 emission factors, (e) CO_2 emissions, (f) CO emission factors, and (g) CO emissions. The grassland ($0\% \leq PTC \leq 10\%$) statistics are shown at PTC = 5%. The woodland (PTC>10%) statistics are defined over 5% PTC intervals.

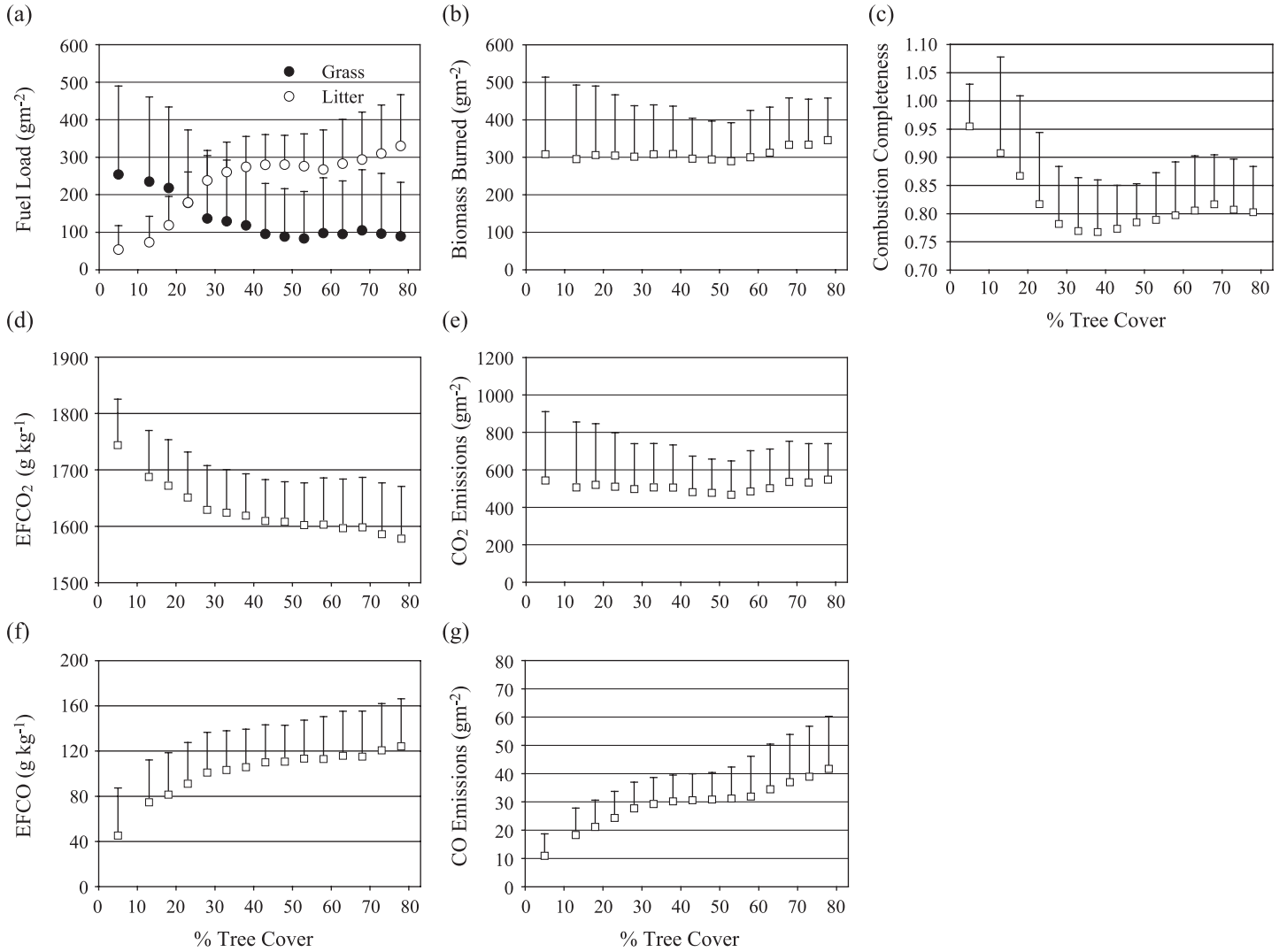

Fig. 10. Mean (symbol) and 1 S.D. statistics computed from the southern Africa, September 2000, GLOBSCAR burned area pixels of (a) fuel load, (b) biomass burned, (c) combustion completeness, (d) CO_2 emission factors, (e) CO_2 emissions, (f) CO emission factors, and (g) CO emissions. The grassland ($0\% \leq PTC \leq 10\%$) statistics are shown at PTC = 5%. The woodland (PTC>10%) statistics are defined over 5% PTC intervals.

8a, 9a, and 10a, and is well documented for southern African savannas (Frost, 1996; Scholes et al., 2002).

The average biomass burned density in woodlands in MODIS is very similar up to 40% PTC and decreases slightly afterwards (Fig. 8b). This is the outcome of the combined—and, in most cases, canceling—effects of the total fuel load density and the combustion completeness in the woodland locations mapped by MODIS (Fig. 8a and c). In general, total fuel load density increases up to about 40% PTC from an average of about 297 to 370 g m^{-2}. At the same time, the combustion completeness decreases from an average of about 0.92 to 0.76. For PTC values higher than 40% the total fuel load density decrease up to about 70% PTC and increase again at higher PTC values, while combustion completeness increases slightly up to 65% and decreases after that.

The average biomass burned density in woodlands in GBA-2000 shows similar distribution and values (Fig. 9b) with MODIS (Fig. 8b) up to 65% PTC. At higher PTC values, slightly more biomass is consumed per unit area in GBA-2000 compared with MODIS due to higher fuel load densities (Figs. 8a and 9a) and higher combustion completeness values (Figs. 8c and 9c). Despite the higher litter loads per unit area in GBA-2000 (Fig. 9a) compared with MODIS (Fig. 8a) at PTC values greater than 65%, the higher combustion completeness occurs because of the smaller contribution of the twigs to the total fuel load per unit area.

The general trend observed in the GLOBSCAR woodland biomass burned densities is that they are slightly higher compared with MODIS and GBA-2000 up to 40% with somewhat larger differences occurring between 40% and 75% (Figs. 8b, 9b, and 10b). This is mainly because of the increased grass contribution in the fuel load mixture (Figs. 8a, 9a, and 10a) at that PTC range, resulting in higher fuel consumption by the fires (Figs. 8c, 9c, and 10c). The average biomass burned consumed per unit area in woodlands in GLOBSCAR is very similar up to about 65% PTC and increases slightly afterwards, again as a net effect of opposite changing total fuel load densities and combustion completeness (Fig. 10a and c). At the regional level, the majority of the burned biomass in woodlands occurs at PTC values below 50% (Fig. 7a). Considering that the biomass burned density values in woodlands for each burned area product are more or less similar across PTC values below 50%, we conclude that biomass burned density is not a significant source of variation for emissions from woodland fires at the regional level. We need to emphasize, though, that this is the case only for the specific month and year of study. Examination of seasonal and interannual differences in the burned area distribution in woodlands among the three products may yield different results.

For all burned area products, the $EFCO_2$ decreases somewhat with increasing PTC by a maximum of about 10% in MODIS and GBA-2000 and 7% in GLOBSCAR (Figs. 8d, 9d, and 10d). Therefore, the CO_2 emission densities in woodlands closely follow the trends of the biomass burned (Figs. 8e, 9e, and 10e). CO_2 emissions per unit area from woodland fires in GLOBSCAR are generally higher than the correspondent CO_2 emissions in MODIS and GBA-2000. There is a pronounced increase in CO emission densities with increasing PTC, which is linked to the increase in EFCO (Figs. 8f, 9f, and 10f). Average CO emission densities increase by maximum factors of 1.9 in MODIS, 3.1 in GBA, and 2.3 in GLOBSCAR (Figs. 8g, 9g, and 10g). This is due to the decreasing contribution of grasses to the fuel bed with increasing PTC and the more smoldering combustion of the woody components in the fuel.

Grassland burns have higher combustion completeness than woodland burns in all burned area products, which is the main reason for the generally higher average biomass burned densities in the MODIS and GBA-2000 grasslands compared with the woodlands (Figs. 8c, 9c, and 10c). In GLOBSCAR, as a result of the lower fuel loads in grasslands compared with woodlands, comparable amounts of biomass are burned per unit area in both land cover types. Consequently, the net effect at the regional level is that slightly more biomass is burned in woodlands than in grasslands, relative to their correspondent burned area ratio (Tables 3 and 7). Field studies have also shown higher combustion completeness in grassland compared with woodland fires and increasing combustion completeness as the dry season progresses (Hoffa et al., 1999; Shea et al., 1996). It is also apparent that the $EFCO_2$ (Figs. 8d, 9d, and 10d) is higher for these very efficient, mostly dry, grassland fires compared with woodland fires. More CO_2/CO is released per unit area in grasslands compared with woodlands in all burned area products (Figs. 8e/g, 9e/g, and 10e/g). The EFCO (Figs. 8f, 9f, and 10f) in grasslands is lower by up to a factor of 2 compared with EFCO in woodlands. The differences in EFCO, rather than the differences in biomass burned, is the fundamental reason for the significantly lower CO emission densities in grasslands compared with woodlands (Figs. 8g, 9g, and 10g).

The emissions profile for woodland and grasslands fire predicted from our model, regardless of the satellite burned area product used, is supported by the general fire emission patterns for these two land cover types in the late dry season when fuel types are fairly dry (Korontzi et al., 2003b; Sinha et al., 2003; Ward et al., 1996; Yokelson et al., 2003) Dry savanna fires, including grasslands and woodlands, are typically efficient fires that have higher emission factors for fully oxidized species, such as CO_2 and NO_x, compared with forest fires (Andreae, 1997; Andreae & Merlet, 2001). At the same time, within the savanna vegetation continuum formations, ranging from pure grasslands to closed-canopy woodlands, there is great variability in fuel composition, which, among other important factors such as fuel condition (e.g., moisture content, packing density) and environmental conditions (e.g., relative humidity, wind direction, and wind speed), determine the relative proportions of flaming and smolder-

ing combustion. Combustion of predominantly grass fuel in grasslands favors the generation of fully oxidized products, such as CO_2 and NO_x. On the other hand, the leaf litter and twig components in the woodland fuel beds tend to involve more smoldering combustion, compared with the grass, favoring the generation of products of incomplete combustion. As the amount of combustible litter increases and the amount of grass decreases, the emission factors for products of incomplete combustion generally increase. The results presented above verify that our emissions model responds in a reasonable fashion to different burned area inputs. Furthermore, they explain why the regional emissions of smoldering compounds from woodland fires are disproportionally high relative to their burned areas for each burned area product.

The aforementioned analysis on the impact of the spatial distribution on emission densities provides the basis to also understand the disproportionate response of emissions for certain atmospheric species to changes in the burned area amounts at the regional level. This nonlinear response is related to the differences in the relative proportion and location of woodland and grassland burns mapped in each product. The main underlying reason is that variations in fuel composition lead to different fire behaviors in these two land cover types, involving more smoldering combustion in woodlands compared with grasslands. The differences in the relative amounts among the different atmospheric species are related to the fact that they are emitted at different molar ratios.

Fig. 11 illustrates that regional average fuel loads, combustion completeness, $EFCO_2$, and EFCO for grasslands and woodlands are comparable among burned area products. However, at the regional level, MODIS maps a higher percentage of burned area and biomass for woodland fires compared with GBA-2000 (Tables 3 and 7). Since burning in woodlands involves more smoldering compared with grasslands (Fig. 11d), the increase of the MODIS over the GBA-2000 is proportionally higher for products of incomplete combustion than the corresponding increase for the fully oxidized emissions products, such as CO_2 and NO_x. The opposite is found when comparing MODIS with GLOBSCAR. MODIS maps a higher proportion of grasslands compared with GLOBSCAR. As seen above, burning in grasslands at the end of the dry season favors emissions of fully oxidized products, such as CO_2 and NO_x. Therefore, the increase in burned area of MODIS over GLOBSCAR results in proportionally larger differences for products of complete combustion compared with products of incomplete combustion. Variations in the fuel load amounts, between woodlands and grasslands, and between the respective woodland and grassland locations mapped in each burned area, appear to be of lesser importance at the regional level.

To assess the sensitivity of the emissions estimation process to different PTC thresholds, we quantified CO_2 and

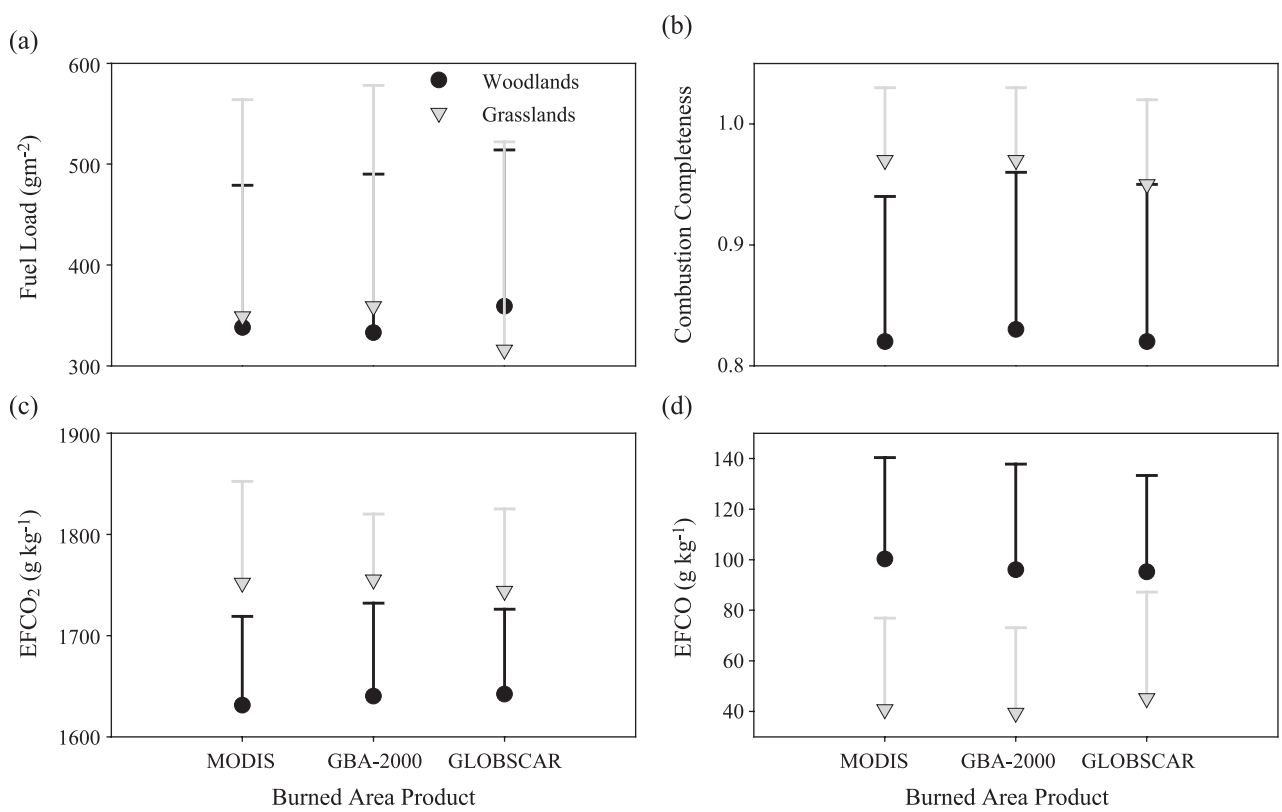

Fig. 11. Mean (symbol) and 1 S.D. statistics computed from southern Africa, September 2000. MODIS, GBA-2000, and GLOBSCAR burned area products for (a) fuel load, (b) combustion completeness, (c) CO_2 emission factors, and (d) CO emission factors.

Table 8
Regional emissions estimates for different PTC thresholds for the grasslands–woodlands classification

Regional emissions (Gg)	5% PTC	15% PTC
MODIS		
CO_2	133,369	134,279
CO	6072	5626
GBA-2000		
CO_2	89,828	90,690
CO	3561	3215
GLOBSCAR		
CO_2	30,213	30,455
CO (Gg)	1438	1334

CO emissions using 5% and 15% PTC values to distinguish between grasslands–woodlands for each burned area product. As seen in Table 8, insignificant differences in the emissions estimates arise at the regional level as a result of applying the different thresholds. It is also conspicuous that the differences in emissions among burned area products are considerable and that they follow the same trends as with the 10% PTC used in the analysis above (Tables 4–6).

The results of this study indicate that reliable information on the burned area spatial distribution, in addition to the amount, is required to increase the accuracy of emissions models. Approaches designed to obtain burned area error information and patterns should be at least ecosystem-specific. Development of increasingly sophisticated and more robust emissions modeling frameworks will require spatially explicit uncertainty measures of burned area. Furthermore, the results suggest that emissions estimation based on extrapolations of the burned area amounts without spatially explicit consideration of the impact of the fuel characteristics on emissions (e.g., approaches that use average emission factors for savanna burning) will result in various degree of uncertainty for different atmospheric species. Obviously, accurate fuel load information is pertinent to the spatial distribution of burned area and their complex interrelation and associated impact on emissions quantification need to be explored further.

3.3. Implications of the spatial distribution of burned area for national emissions

Party countries to the United Nations Framework Convention on Climate Change (UNFCC) are obliged to report their national greenhouse gas emissions, including those from savanna burning (Braatz et al., 1995). The spatial differences in the burned area products discussed in the

Table 9
Intercomparison of the MODIS, GBA-2000, and GLOBSCAR burned area and emissions for selected trace gases and $PM_{2.5}$ per country, southern Africa, September 2000

Country	MODIS area ($km^2 \times 10^2$)	GBA-2000 area ($km^2 \times 10^2$)	GLOBSCAR area ($km^2 \times 10^2$)	MODIS CO_2 (Tg)	GBA-2000 CO_2 (Tg)	GLOBSCAR CO_2 (Tg)	MODIS CO (Gg)	GBA-2000 CO (Gg)	GLOBSCAR CO (Gg)
Angola	444.9	333.1	118.9	29.824	24.707	6.461	907.11	632.74	314.33
Botswana	70.1	59.5	5.9	4.749	4.006	0.417	92.83	77.72	9.14
Burundi	2.6	0.8	0.9	0.102	0.035	0.041	4.81	1.09	1.96
Malawi	25.5	20.2	3.2	1.112	0.968	0.144	60.03	49.34	9.56
Mozambique	636.4	323.5	116.3	27.789	13.548	5.560	1517.33	742.85	266.77
Namibia	150.6	128.7	5.0	10.163	8.506	0.296	195.36	162.06	5.42
Rwanda	0.3	0.4	0.3	0.012	0.014	0.011	0.77	0.47	0.65
South Africa	263.1	198.6	107.3	13.230	10.010	5.296	389.22	294.72	169.85
Swaziland	3.3	1.9	2.4	0.173	0.098	0.132	6.85	4.03	5.63
Tanzania	128.0	125.5	31.4	5.106	5.162	1.447	324.55	237.96	82.94
Zambia	722.7	333.6	71.2	29.633	13.298	3.021	1810.36	804.11	186.05
Zimbabwe	131.5	78.4	37.1	7.623	4.474	2.574	266.12	147.40	84.06
Others	106.0	126.8	98.1	4.264	5.431	4.918	291.43	236.91	256.63

Country	MODIS CH_4 (Gg)	GBA-2000 CH_4 (Gg)	GLOBSCAR CH_4 (Gg)	MODIS NMHC (Gg)	GBA-2000 NMHC (Gg)	GLOBSCAR NMHC (Gg)	MODIS $PM_{2.5}$ (Gg)	GBA-2000 $PM_{2.5}$ (Gg)	GLOBSCAR $PM_{2.5}$ (Gg)
Angola	23.174	13.823	10.322	25.116	17.698	8.567	75.271	43.880	34.431
Botswana	1.590	1.319	0.170	2.385	1.992	0.252	5.423	4.507	0.540
Burundi	0.153	0.026	0.063	0.137	0.034	0.055	0.499	0.077	0.204
Malawi	2.083	1.680	0.359	1.611	1.316	0.249	7.042	5.687	1.234
Mozambique	52.474	25.759	8.693	40.723	19.919	7.319	177.131	87.018	28.882
Namibia	3.392	2.787	0.089	4.875	4.013	0.131	11.926	9.867	0.322
Rwanda	0.028	0.012	0.024	0.022	0.014	0.017	0.092	0.037	0.082
South Africa	9.508	7.248	4.426	11.195	8.431	4.864	29.885	22.914	14.057
Swaziland	0.204	0.124	0.175	0.192	0.110	0.154	0.667	0.413	0.581
Tanzania	11.892	7.761	2.906	8.712	6.693	2.291	40.363	25.578	9.693
Zambia	65.504	28.966	6.752	47.958	21.398	4.949	223.256	98.502	22.980
Zimbabwe	7.069	3.798	2.084	7.844	4.324	2.524	21.919	11.784	6.281
Others	11.019	7.458	8.746	7.625	6.701	6.958	37.821	24.323	29.231

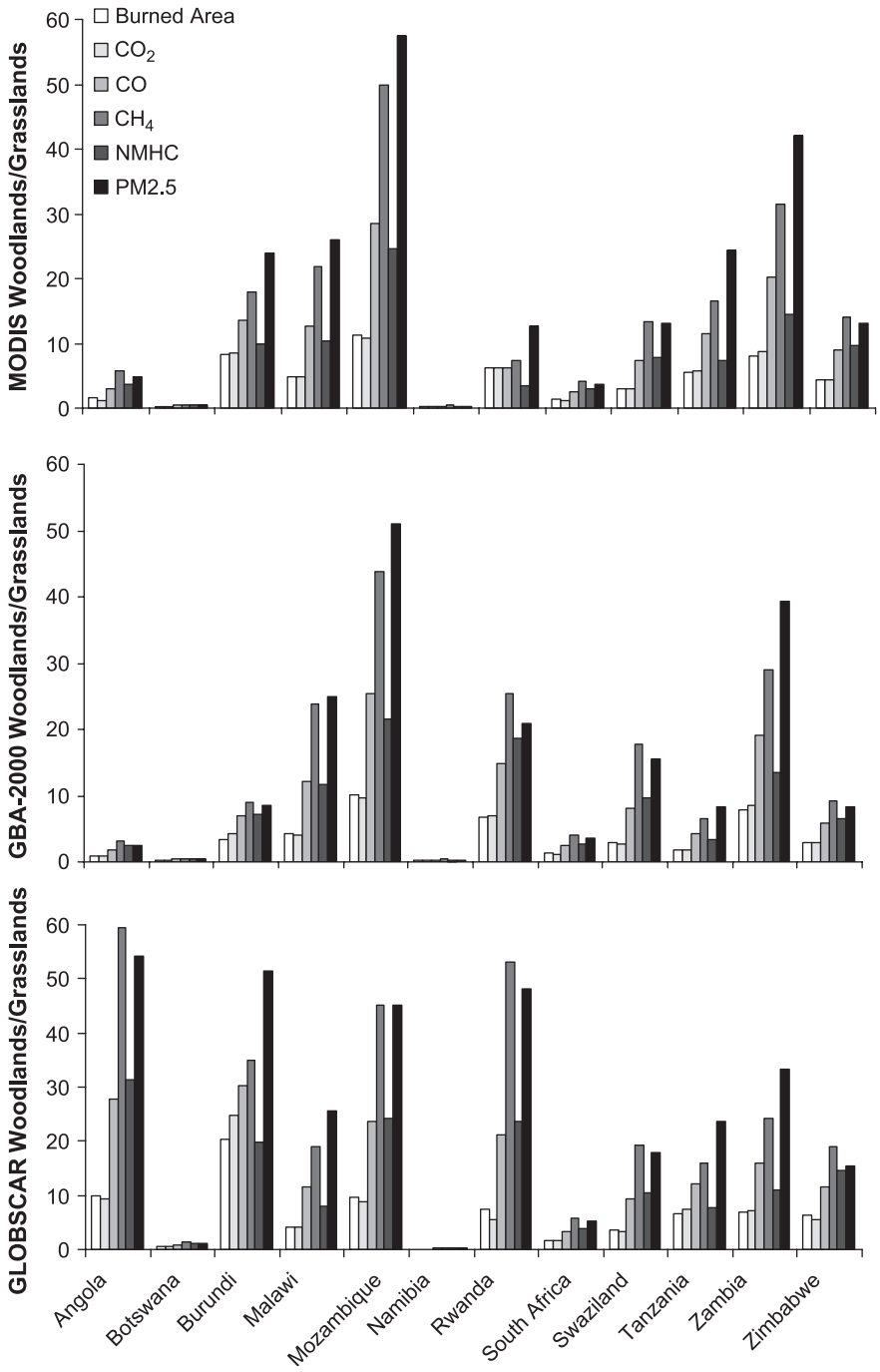

Fig. 12. MODIS, GBA-2000, and GLOBSCAR woodland over grassland burned area ratios and selected trace gas and particulate emissions for September 2000. Only those southern African countries situated completely south of the equator are reported.

previous section become especially important within this context, since some countries might be more susceptible to these uncertainties in the burned area mapping than others. We limit the discussion to larger countries since emission estimates for small countries have likely higher uncertainties. Table 9 lists the country-level burned area and emis-

Table 10
Average values and (± 1 S.D.) of fuel load (g m^{-2}), combustion completeness (CC), and emission factors (EF) (g kg^{-1}) for woodland fires in Tanzania, September 2000, using MODIS and GBA-2000

	Fuel load	CC	$EFCO_2$	EFCO	$EFCH_4$	EFNMHC	$EFPM_{2.5}$
MODIS	317 (155)	0.78 (0.16)	1587 (104)	120.1 (47.4)	4.646 (2.469)	3.028 (0.936)	16.198 (9.243)
GBA-2000	297 (179)	0.81 (0.18)	1607 (114)	110.9 (51.8)	4.168 (2.697)	2.847 (1.022)	14.409 (10.098)

Table 11
Average values and ($\pm \sigma$) of fuel load (g m^{-2}), combustion completeness (CC), and emission factors (EF) (g kg^{-1}) for grassland fires in Tanzania, September 2000, using MODIS and GBA-2000

	Fuel load	CC	$EFCO_2$	EFCO	$EFCH_4$	EFNMHC	$EFPM_{2.5}$
MODIS	241 (182)	0.94 (0.06)	1685 (126)	75.2 (64.9)	2.169 (2.474)	3.335 (3.800)	4.716 (4.319)
GBA-2000	250 (183)	0.95 (0.07)	1715 (110)	60.3 (56.8)	1.600 (2.166)	2.462 (3.326)	3.724 (3.782)

sions for selected trace gases and particulates for the three burned area products. Fig. 12 illustrates the corresponding woodland to grassland ratios for the three burned area products.

As can be seen in the case of Tanzania, despite the practically equal MODIS and GBA-2000 burned area amounts, the MODIS-derived estimates for products of incomplete combustion are higher by approximately 30–58%. The differences are primarily due to the fact that MODIS maps more burns in woodlands compared with GBA-2000. The ratio of woodland over grassland fires mapped in MODIS is 5.5, whereas it is 1.9 in GBA-2000. The variations in fuel load, combustion completeness, and emission factors between woodlands and grasslands primarily, and between the respective woodland and grassland locations mapped in each burned area product secondarily, result in these differences in emissions. In the MODIS-driven emissions model, the average values for woodlands and grasslands in Tanzania are 317 and 241 g m^{-2} for fuel load, 0.78 and 0.94 for combustion completeness, 1587 and 1685 g kg^{-1} for emission factors for CO_2, 120.1 and 75.2 g kg^{-1} for emission factors for CO, 4.646 and 2.169 g kg^{-1} for emission factors for CH_4, 3.028 and 3.335 g kg^{-1} for emission factors for NMHC, and 16.198 and 4.716 g kg^{-1} for emission factors for $PM_{2.5}$, respectively (Tables 10 and 11).

In comparison, the GBA-2000-driven average values for woodlands and grasslands in Tanzania are 297 and 250 g m^{-2} for fuel load, 0.81 and 0.95 for combustion completeness, 1607 and 1715 g kg^{-1} for emission factors for CO_2, 110.9 and 60.3 g kg^{-1} for emission factors for CO, 4.168 and 1.600 g kg^{-1} for emission factors for CH_4, 2.847 and 2.462 g kg^{-1} for emission factors for NMHC, and 14.409 and 3.724 g kg^{-1} for emission factors for $PM_{2.5}$, respectively (Tables 10 and 11). In other countries where major biomass burning occurs, such as Mozambique, differences in emissions closely follow the differences in burned area amounts because of the similar woodland-over-grassland ratios in MODIS (11.2) and GBA-2000 (10.0) for this country and the similar fuel load distribution.

4. Conclusions

This sensitivity study contributes to a better understanding of the relationship between the spatial distribution of burned areas and emissions. The model's predictions, regardless of the burned area product, are consistent with published field studies of emission patterns from woodland and grassland fires (Hoffa et al., 1999; Ward et al., 1996). These published studies show that burning in woodlands favors emissions of products of incomplete combustion compared with grasslands. Changes in the spatial distribution of burning and the total burned area cause significant changes in the emissions output. Due to the different emission profiles in woodlands and grasslands, these changes are not necessarily proportional to the differences in the total burned area. The nonlinearity of emissions to burned area highlights that Eq. (1) should be applied within a spatially explicit context and that simple extrapolations based on burned area amounts can lead to different uncertainties for different emissions products. Information on the spatial distribution of burned area is essential to reducing uncertainty in emissions estimates. Validation of burned area datasets is a priority for satellite data providers, for a variety of usages, including reduction of emissions models uncertainties. There is some urgency for the international satellite community to develop the appropriate protocols and procedures for land data product validation (Justice et al., 2002b; Morisette et al., 2002). From an emissions modeling perspective, spatially explicit maps of burned area uncertainty are desirable since the spatial distribution of the burning has significant implications for emissions quantification. This information is pertinent not only for improvement of the satellite burned area products, but it will also provide the base information for proper capture of uncertainty in emissions models. Furthermore, this will enable emission uncertainties to be defined with respect to different landscape units, including countries, in support of greenhouse gas emissions reporting. Failing the availability of spatially explicit uncertainty information, our results indicate that ecosystem-specific uncertainty information will provide a step forward. Even though we focused on one month at the end of the 2000 dry season, it is very likely that uncertainty in the burned area also varies through time and should also be quantified within the context of seasonal emissions modeling (Korontzi et al., 2003a).

Acknowledgements

This study was carried out as part of SAFARI-2000. Funding in partial support of this research was provided by National Aeronautics and Space Administration (NASA) grants NAS-531365 and NAG-511251. Stefania Korontzi is also supported by the NASA's Earth System Graduate Research Fellowship. The anonymous reviewers are thanked for their helpful comments.

References

Andreae, M. O. (1997). Emissions of trace gases and aerosols from southern African savanna fires. In B. W. Van Wilgen, M. O. Andreae, J. G. Goldammer, & J. A. Lindesay (Eds.), *Fire in southern African savannas: Ecological and atmospheric perspectives* (pp. 161–183). Johannesburg, South Africa: Witwatersrand Univ. Press.

Andreae, M. O., & Merlet, P. (2001). Emissions of trace gases and aerosols from biomass burning. *Global Biogeochemical Cycles*, *15*, 955–966.

Bertschi, I., Yokelson, R. J., Ward, D. E., Babbitt, R. E., Susott, R. A., Goode, J. G., & Hao, W. M. (2003). Trace gas and particle emissions from fires in large diameter and belowground biomass fuels. *Journal of Geophysical Research*, *108*(D13), 8472 (doi:10.1029/2002JD002100).

Braatz, B. V., Brown, S., Isichei, A. O., Odada, E. O., Scholes, R. J., Sokona, Y., Drichi, P., Gaston, G., Delmas, R., Holmes, R., Amous, S., Muyungi, R. S., De Jode, A., & Gibbs, M. (1995). African greenhouse gas emission inventories and mitigation options: Forestry, land-use change, and agriculture. *Environmental Monitoring and Assessment*, *38*, 109–126.

Dikshit, O., & Roy, D. P. (1996). An empirical investigation of image resampling effects upon the spectral and textural information content of a high spatial resolution multispectral image. *Photogrammetric Engineering and Remote Sensing*, *62*, 1085–1092.

Dwyer, E., Pereira, J. M. C., Grégoire, J. -M., & DaCamara, C. C. (2000). Characterization of the spatio-temporal patterns of global fire activity using satellite imagery for the period April 1992 to March 1993. *Journal of Biogeography*, *27*(1), 57–69.

Eva, H., & Lambin, E. F. (1998). Burnt area mapping in Central Africa using ATSR data. *International Journal of Remote Sensing*, *19*, 3473–3497.

Frost, P. G. H. (1996). The ecology of miombo woodlands. In B. Campbell (Ed.), *The miombo in transition: Woodlands and welfare in Africa* (pp. 11–58). Bogor, Indonesia: CIFOR.

Frost, P. G. H., & Robertson, F. I. (1987). The ecological role of fire in savannas. In B. H. Walker (Ed.), *Determinants of tropical savannas* (pp. 93–140). Oxford: IRL Press.

Food and Agriculture Organization of the United Nations. (2001). Global forest resources assessment 2000 (FRA 2000): Appendix 2. Terms and definitions. *FAO forestry paper, vol. 140* (pp. 363–370). Rome: Food and Agriculture Organization of the United Nations.

Grégoire, J. -M., Tansey, K., & Silva, J. M. N. (2003). The GBA-2000 initiative: Developing a global burned area database from SPOT VEGETATION imagery. *International Journal of Remote Sensing*, *24*, 1369–1376.

Guenther, B., Xiong, X., Salomonson, V. V., Barnes, W. L., & Young, J. (2002). On-orbit performance of the earth observing system Moderate Resolution Imaging Spectroradiometer; first year of data. *Remote Sensing of Environment*, *83*, 16–30.

Hansen, M. C., DeFries, R. S., Townshend, J. R. G., Carroll, M., Dimiceli, C., & Sohlberg, R. (2003). The MODIS 500 meter global vegetation continuous field products. *Second international workshop on the analysis of multitemporal remote sensing images, Ispra, Italy*, in press.

Hansen, M. C., DeFries, R. S., Townshend, J. R. G., Sohlberg, R., Dimiceli, C., & Carroll, M. (2002). Towards an operational MODIS continuous field of percent tree cover algorithm: Examples using AVHRR and MODIS data. *Remote Sensing of Environment*, *83*(1–2), 303–319.

Hély, C., Caylor, K. K., Dowty, P. R., Swap, R. J., & Shugart, H. H. (2003a). SAFARI 2000 Modeled Fuel Load in Southern Africa 1999–2000. In J. Nickeson, D. Landis, & J.L. Privette (Eds.), *SAFARI 2000 CD-ROM Series, vol. 3*. CD-ROM. National Aeronautics and Space Administration, Goddard Space Flight Center, Greenbelt, Maryland, USA. Available from Oak Ridge National Laboratory Distributed Active Archive Center, Oak Ridge, Tennessee, USA, http://www.daac.ornl.gov/

Hély, C., Dowty, P. R., Alleaume, S., Caylor, K. K., Korontzi, S., Swap, R. J., Shugart, H. H., & Justice, C. O. (2003b). Regional fuel load for two climatically contrasting years in southern Africa. *Journal of Geophysical Research*, *108*(D13), 8475 (doi:10.1029/2002JD002341).

Hoffa, E. F., Wakimoto, R. H., Ward, D. E., Hao, W. M., & Susott, R. A. (1999). Seasonality of carbon emissions from biomass burning in a Zambian savanna. *Journal of Geophysical Research*, *104*, 13841–13853.

Intergovernmental Panel on Climate Change (IPCC) (1997). *Revised 1996 IPCC Guidelines for National Greenhouse Gas Inventories Workbook*, *2*, 4.23–4.28.

Justice, C. O., Giglio, L., Korontzi, S., Owens, J., Morisette, J. T., Roy, D. P., Descloitres, J., Alleaume, S., Petitcolin, F., & Kaufman, Y. (2002a). The MODIS fire products. *Remote Sensing of Environment*, *83*(1–2), 244–262.

Justice, C. O., Malingreau, J. P., & Setzer, A. (1993). Satellite remote sensing of fires: Potential and limitation. In P. J. Crutzen, & J. G. Goldammer (Eds.), *Fire in the environment. The ecological, atmospheric, and climatic importance of vegetation fires* (pp. 77–88). Chichester: Wiley.

Justice, C. O., Townshend, J. R. G., Vermote, E. F., Masuoka, E., Wolfe, R. E., Saleous, N., Roy, D. P., & Morisette, J. T. (2002b). An overview of MODIS Land data processing and product status. *Remote Sensing of Environment*, *83*(1–2), 3–15.

Korontzi, S., Justice, C. O., & Scholes, R. J. (2003a). Influence of timing and spatial extent of vegetation fires in southern Africa on atmospheric emissions. *Journal of Arid Environments*, *54*(2), 395–404.

Korontzi, S., Ward, D. E., Susott, R. A., Yokelson, R. J., Justice, C. O., Hobbs, P. V., Smithwick, E., & Hao, W. M. (2003b). Seasonal variation and ecosystem dependence of emission factors for selected trace gases and $PM_{2.5}$ for southern African savanna fires. *Journal of Geophysical Research*, *108*(D24), 4758 (doi:10.1029/2003JD003730).

Morisette, J. T., Privette, J. L., & Justice, C. O. (2002). A framework for the validation of MODIS land products. *Remote Sensing of Environment*, *83*(1–2), 77–96.

Piccolini, I. (1998). Development and validation of an adaptive algorithm for burn scar detection using ERS/ATSR-2 data. *PhD Thesis*, Univ. La Sapienza, Rome, Italy.

Robinson, J. M. (1991). Fire from space: Global fire evaluation using infrared remote sensing. *International Journal of Remote Sensing*, *12*(1), 3–24.

Roy, D. P. (2003). SAFARI 2000 July and September MODIS 500 m Burned Area Products for Southern Africa. In J. Nickeson, D. Landis, & J. L. Privette, (Eds.), *SAFARI 2000 CD-ROM Series, vol. 3*. CD-ROM. National Aeronautics and Space Administration, Goddard Space Flight Center, Greenbelt, Maryland, USA. Available from Oak Ridge National Laboratory Distributed Active Archive Center, Oak Ridge, Tennessee, USA, http://www.daac.ornl.gov/

Roy, D. P., Borak, J., Devadiga, S., Wolfe, R., Zheng, M., & Descloitres, J. (2002a). The MODIS land product quality assessment approach. *Remote Sensing of Environment*, *83*, 62–76.

Roy, D. P., Frost, P. G. H., Justice, C. O., Landmann, T., Le Roux, J. L., Gumbo, K., Makungwa, S., Dunham, K., Du Toit, R., Mhwandagara, K., Zacarias, A., Tacheba, B., Dube, O. P., Pereira, J. M. C., Mushove, P., Morisette, J. T., Santhana Vannan, S. K., & Davies, D. (2004). The Southern Africa Fire Network (SAFNet) regional burned area product validation protocol. *International Journal of Remote Sensing*, (in press).

Roy, D. P., & Landmann, T. (2004). Characterizing the surface heterogeneity of fire effects using multi-temporal reflective wavelength data. *International Journal of Remote Sensing* (in press).

Roy, D. P., Lewis, P., & Justice, C. O. (2002b). Burned area mapping using multi-temporal moderate spatial resolution data—A bi-directional reflectance model-based expectation approach. *Remote Sensing of Environment*, *83*, 263–286.

Roy, D. P., Yufang, J., Justice, C. O., Giglio, L., & Lewis, P. E. (2003). Multi-year southern Africa MODIS burned area product generation and validation, Fall AGU meeting, San Francisco, December 8–12, 2003, Presented in session, "Validation and Application of Land Surface Products from the MODIS Sensor". *Eos, Transactions, AGU*, *84*(46) (Abstract B22E-02).

Scholes, M. C., & Andreae, M. O. (2000). Biogenic and pyrogenic emissions from Africa and their impact on global atmosphere. *Ambio*, *29*, 23–29.

Scholes, R. J., Dowty, P. R., Caylor, K. K., Parsons, D. A. B., Frost, P. G. H., & Shugart, H. H. (2002). Trends in savanna structure and composition along an aridity gradient in the Kalahari. *Journal of Vegetation Science*, *13*, 419–428.

Scholes, R. J., Ward, D. E., & Justice, C. O. (1996). Emissions of trace gases and aerosol particles due to vegetation burning in southern hemisphere Africa. *Journal of Geophysical Research*, *101*(D19), 23677–23682.

Seiler, W., & Crutzen, P. J. (1980). Estimates of gross and net fluxes of carbon between the biosphere and the atmosphere from biomass burning. *Climatic Change*, *2*(3), 207–247.

Shea, R. W., Shea, B. W., Kauffman, J. B., Ward, D. E., Haskins, C. I., & Scholes, M. C. (1996). Fuel biomass and combustion factors associated with fires in savanna ecosystems of South Africa and Zambia. *Journal of Geophysical Research*, *101*(D19), 23551–23568.

Silva, J. M. N., Pereira, J. M. C., Cabral, A. I., Sá, A., Vasconcelos, M. J. P., Mota, B., & Grégoire, J. -M. (2003). An estimate of the area burned in southern Africa during the 2000 dry season using SPOT-VEGETATION. *Journal of Geophysical Research*, *108*(D13), 8498 (doi:10.1029/2002JD002320).

Simon, M., Plummer, S., Fierens, F., Hoelzmann, J. J., & Arino, O. (2004). Burnt area detection at global scale using ATSR-2: The GLOBSCAR products and their qualification. *Journal of Geophysical Research 109*, D14S02 (doi:10.1029/2003JD003622).

Sinha, P., Hobbs, P. V., Yokelson, R. J., Bertschi, I. T., Blake, D. R., Simpson, I. J., Gao, S., Kirchstetter, T. W., & Novakov, T. (2003). Emissions of trace gases and particles from biomass burning in southern Africa. *Journal of Geophysical Research*, *108*(D13), 8487 (doi:10.1029/2002JD002325).

Stroppiana, D., Pinnock, S., Pereira, J. M. C., & Grégoire, J. -M. (2002). Radiometric analysis of SPOT-VEGETATION images for burnt area detection in northern Australia. *Remote Sensing of Environment*, *82*, 21–37.

Swap, R. J., Annegarn, H. J., Suttles, J. T., King, M. D., Platnick, S., Privette, J. L., & Scholes, R. J. (2003). Africa burning: A thematic analysis of the Southern African Regional Science Initiative (SAFARI 2000). *Journal of Geophysical Research*, *108*(D13), 8465 (doi:10.1029/2003JD003747).

Tansey, K., Binaghi, E., Boschetti, L., Brivio, P. A., Cabral, A., Ershov, D., Flasse, S., Fraser, R., Gallo, I., Graetz, D., Grégoire, J. -M., Maggi, M., Peduzzi, P., Pereira, J. M., Sá, A., Silva, J., Sousa, A., Stroppiana, D., & Vasconcelos, M. J. P. (2002). Implementation of regional burnt area algorithms for the GBA-2000 initiative. *European Commission Joint Research Centre, EUR 20532 EN* (p. 159). Publications of the European Commission.

Trollope, W. S. W., Trollope, L. A., Potgieter, A. L. F., & Zambatis, N. (1996). SAFARI-92 characterization of biomass and fire behavior in the small experiment burns in the Kruger National Park. *Journal of Geophysical Research*, *101*(D19), 23531–23540.

Van der Werf, G. R., Randerson, J. T., Collatz, G. J., & Giglio, L. (2003). Carbon emissions from fires in tropical and subtropical ecosystems. *Global Change Biology*, *9*(4), 547–562.

Ward, D. E., Hao, W. M., Susott, R. A., Babbitt, R. E., Shea, R. W., Kauffman, J. B., & Justice, C. O. (1996). Effect of fuel composition on combustion efficiency and emission factors for African savanna ecosystems. *Journal of Geophysical Research*, *101*(D19), 23569–23576.

Yokelson, R. J., Bertschi, I. T., Christian, T. J., Hobbs, P. V., Ward, D. E., & Hao, W. M. (2003). Trace gas measurements in nascent, aged, and cloud-processed smoke from African savanna fires by airborne Fourier transform infrared spectroscopy (AFTIR). *Journal of Geophysical Research*, *108*(D13), 8478 (doi:10.1029/2002JD002322).